Proceedings of the Institution of Mechanical Engineers, Part G:
Journal of Aerospace Engineering, Volume 233, Issue 1, 2019, pp. 261-284
DOI:10.1177/0954410017728968

Original Article

Development of a new method for ATFCM based on trajectory based operations

Dany Gatsinzi, Francisco J Saez Nieto, Irfan Madani

Abstract

This paper discusses a possibility to evolve the current Air Traffic Flow and Capacity Management towards a more proactive approach. This new method focusses on reducing the expected probability of ATC intervention based on "hot spot" identification and mitigation at strategic level by applying subliminal changes on the times of arrival at the crossing or merging points (junctions). The concept is fully aligned with the Trajectory Based Operation principles. The approach assumes that the changes on the times of arrival only demand small speed changes from the involved aircraft. In this study, the hot spots are defined as clusters of aircraft expected to arrive to the junctions. Two aircraft are said to be in the same cluster if their proximity and closure rate are below a given threshold.

School of Aerospace, Transport and Manufacturing, Cranfield University, UK

Corresponding author:
Dany Gatsinzi, School of Aerospace Transport and Manufacturing, Cranfield University, Building 83, College Rd, Cranfield MK43 0AL, United Kingdom.
Email:Dany.Gatsinzi@cranfield.ac.uk
Tel:+447941514458

Some exercises are proposed and solved by applying this method. The obtained results show its ability to remove the potential conflicts by applying simple linear programming.

This approach seeks to change the current capacity limiting factor, established by the number of aircraft occupying simultaneously each sector, to another parameter where the level of traffic complexity, flowing towards junctions, is identified and mitigated at strategic level.

The speed changes, used as the control variable and computed before or during the flight, are designed to provide an adjustment on aircraft's Required Time of Arrival at the junctions in order to have a de-randomized and well-behaved (conflict free) traffic. This will enable improvements in airspace capacity/ safety binomial.

It is recognized that this measure alone is unable to produce a conflict free airspace, and then other collaborative and coordinated actions, such as adjusting and swapping departing times at the departing airports (before the Aircraft are taking off), offsetting some flights from nominal route, and allowing multi-agent separation management (while they are in flight) should be applied together with this method.

Keywords

ATFCM, TBO, CD&R, DCB, junction, TOA, hot spot, complexity

1 Background

The Air Traffic Flow and Capacity Management (ATFCM) has been the object of intensive research, due to the sustained growth of air traffic. It is a required service for managing the balance between air traffic demand and airspace capacity, defined by the ATC operational resources. Since its inception, the Air Traffic Management (ATM) system has undergone several significant changes from a primitive form, based on simple

operational rules, to a complex network supported by sensors, communication and control subsystems.[1] In addition, the evolution of the technical enablers such as radio communication, navigational aids (Navaids) and radar systems which revolutionised the way ATM system was operating in 1950s, still forms the backbone of the current system.[1] Derived from those supporting technologies, today's ATM system is still basically based on a network of fixed routes and ATC sectors.

To achieve the required levels of safety for air traffic across this network, a human supervisory control system is applied. The process is based on air traffic controllers (ATCOs) detecting and solving aircraft (A/C) conflicts within each ATC sector in a reactive manner. The conventional airspace organization, which is constituted of a network of fixed routes, sectors and nodes, enables the ATCOs to have a priori information on the potential A/C conflicts since they are typically located at the crossing/merging points of the route network. The number of simultaneous A/C that can be handled within a sector is limited; saturating the ATCO's capacity. To maintain an acceptable controller workload, a maximum allowable number of simultaneous A/C within a sector is defined, regardless of their particular complexity. The result is that the current airspace capacity then strongly depends on the individual capacity of each ATC sector. The workload being experienced by ATCOs is the main limiting factor of the whole airspace capacity; and the current ATM operations are commonly referred to as "airspace based operations".

At present, airspace resources are used to attend demand, while they suffer from idleness and saturations that foster regulations and holdings, which causes inefficient flight trajectories.

The above-mentioned situation is more significant in high traffic density airports and ATC sectors in Europe and it results into unnecessary delays. According to the Eurocontrol Performance Review Report (2016),[2] considering only the ATFM en-route delays, an average of 51seconds delay per flight and a total of 8.7million minutes delay were recorded in the ECAC area, resulting in en-route ATFM delay costs estimated at 8.7million Euro. In addition to these substantial delay costs, the projected rising demand for air travel has the potential to further increase air traffic congestion and reduce the ATM operational safety and efficiency.[3] With the increase of traffic congestion in ATC sectors, the Air Traffic Controllers' workload, which mainly increases due to increased number of tactical actions required to remove conflicts between aircraft also increases, limiting the number of operations that can be attended safely and efficiently by the controller.[4]

To overcome these limitations, SESAR, a European ATM joint-research program,[5] as well as its counterpart NextGen in the United States,[6] are actively researching and proposing procedures to minimise the problems. A key common pillar of both projects is the "Trajectory Based Operations (TBO)" based on the 4D trajectory concept, where A/C are expected to fly closely to their own preferred trajectories whilst meeting the performance requirements defined associated to the procedure flown. Under this TBO principle, all ATM stakeholders will collaboratively define these trajectories. Constraints associated to ATFCM will then be solved under the principle of obtaining trajectories that suits users' internal business objectives.[7]

The aforementioned performance requirements, which are defined in ICAO's Performance Based Navigation (PBN), allow A/C to navigate their flights following a

planned centered-line trajectory accurately either under “Free Routing” (FR) airspace or following the conventional route structure. The application of FR changes the current fixed and well defined “crossing points”, where most of the conflicts are expected to occur. In FR, the number of junctions is increased and then, for the same population, the number of aircraft crossing them will be, on average, reduced. However, the complexity of the airspace might be increased. In addition, the workload for the air traffic controllers to detect the conflicts, as they are broadly distributed, could be increased.

The air traffic flow management optimization problems have been intensively addressed over the years. The models developed to adapt demand and capacity can be classified as:

- Macroscopic approaches ;
- Microscopic approaches.

Currently, macroscopic approaches are usually applied to wide geographical areas providing corrective measures before the A/C is flying. They use aggregated flight plans as the input, and the ATC sectors’ and airports’ capacities as the “limiting factor”. Throughout a demand capacity balancing (DCB) dynamic exercise, the initial flight plans can be directly approved or “regulated”. The regulation action is then the available “control action” and in Europe, this usually implies limiting the maximum rate of aircraft entering either a regulated volume of airspace or airport by modifying flight plans, agreed between Flight Operating Centres (FOC) and Network Manager (NM), which may either involve rerouting (new A/C trajectory) or assigning new take-off times through ATFM time slots.

The ground holding is the most common regulation criteria. The "ground delay problem (GDP)" seeks to minimize the sum of airborne and ground delay costs when the demand exceeds the allowed capacity. The GDP problem has been studied in a simple airport capacity constrained scenario, [8] and in a more complex scenario involving capacities of a network of interconnected airports and connecting flights while considering cascading effect of delays on flights in the network. [9] In both scenarios, the airspace (ATC Sector(s)) capacity was assumed unconstrained, and speed control and rerouting were not considered as possible solutions. In a congested airspace such as that over Europe, these assumptions are idealistic.

To remove this unrealistic airspace capacity assumption, a deterministic programing model was developed to solve the ATFCM problem considering the full network capacity constraints (airports' and en-route sectors' capacity constraints). [10] For each A/C in the network, the model finds optimal departure and sector occupancy time that minimises the total network delay. The authors concluded that the problem is NP-hard and suggested a heuristic which proved to be computationally efficient. This model however, also does not allow for rerouting and speed changes as control variables. A more complete model that allows rerouting has been recently developed. [11] This model has been validated on large-scale traffic instances of the size of US National Airspace with viable computational times. Nowadays, this model is the most complete macroscopic description of the ATFCM problem.

Currently, these macroscopic approaches for ATFCM problems are sufficiently powerful to address large-scale scenarios in which A/C trajectories are represented as

aggregated flow, but they are not able to account for the effects of potential conflicts that may arise from individual planned trajectories on the ATCO's workload.

Flow management microscopic approaches are currently focused on conflict detection and resolution (CD&R), including sequencing, merging and metering when competing for limited resources (such as runways and merging points). The goal is to provide conflict free trajectories for all involved A/C. CD&R algorithms are seldom applied as ATFCM operational solutions to address the airspace capacity problem, whereas they are inherently the common ATCO's reactive/tactical solutions. A comprehensive survey of CD&R algorithms is provided in Kuchar and Yang. [12] Apart from ground or air holdings, three well-known techniques exist that can be applied to remove A/C conflicts; heading, flight level and speed changes. Currently however, conflict resolution by speed control is rarely applied. This is mainly due to the limited possible speed changes, compatible with A/C performance. Speed control requires significant anticipation to be efficient, which is not the case for heading or for flight level changes. Heading and flight level changes can quickly avoid loss of separation than speed control. Consequently, these techniques are more intuitively suitable than speed control and they are paramount under time pressure (reactive situations) to resolve conflicts. This paper focuses on reducing the probability of ATC intervention to resolve conflicts far in advance (at strategic ATFM level) when there is enough anticipation time suitable for speed control actions. These speed changes will be applied to the flight plans (RBT level) as time constrains, for instance, issued in form of RTAs.

A hybrid CD&R model combining speed control and flight level changes has also been proposed by Vela et al., [13] formulated as a Mixed-Integer Linear programme

(MILP), some encouraging results were obtained in the paper. However, the model was implemented with a consideration of the airspace size of only one ATC sector. One of the reasons why speed control was poorly investigated was the lack of accuracy of trajectory predictions. However, the new developments of CNS avionics technology such as the FMS CTA function opens the door to the application of speed control based conflict resolution models.

More recently, several European ATM projects have focused on developing tools to provide strategic trajectories de-confliction functions, exploring the impact of applying time constraints at given waypoints. These tools rely on a key pillar of SESAR Target concept, the "Trajectory Based Operations (TBO)". TBO is based upon the 4D trajectory concept, which describes for each flight, its intended trajectory, defined with a required accuracy associated to all three spatial coordinates (3D) and target times to specific waypoints.[14] The 4DT management evolves out of a collaborative layered planning that spans through different phases. The initial RBT, which is the trajectory airspace user agree to fly and the airports and ANSPs agree to facilitate, is an outcome of the demand capacity balancing process.[14] This RBT is a reference, but it is not required to adhere with specific margins in time or space, unless some initial constrains are added to its specification. The RBT update and revision processes are an integral part of the SESAR concept. Initial RBT is closely related to the ICAO EFPL concept, representing an extension to the conventional ICAO flight plan. It provides the 4D-trajectory description as computed by the flight planning system to generate the operational flight plan; it also provides performance data describing the climbing and descending capabilities specific to the flight.

The improved accuracy associated to the 4DT increases trajectory predictability, this has led to innovative studies on new trajectory de-confliction methods to allow better traffic management processes at different planning layers.

One of them is the "En-Route Air Traffic Soft Management Ultimate System (ERASMUS)".[15,16] Its main objective was to develop a tool to improve A/C ATC strategic de-confliction by generating a conflict-free trajectory segment of 15 minutes look-ahead time for each flight. This was achieved through the Trajectory Control by Speed Adjustment (TC-SA) function, which proposes real-time in-flight adjustments of the RBT based on minor (-6%, -6%) speed adjustments in order to reduce the current ATC workload. These speed changes are referred to as "subliminal".

The ERASMUS strategic de-confliction process assumes the availability of accurate 4D trajectory predictions, where each aircraft downlinks to ground a 4D trajectory every 2 minutes for a look–ahead time of 20 minutes. According to the existing 4D trajectory constraints, this ground processing system is able to update its picture of the traffic situation every 3 minutes and then, its conflict detection and resolution algorithms detects whether or not there are conflicts for the next 15 minutes trajectory segment of each aircraft. For the detected conflicts, new trajectory clearances for the next 15 minutes window are up-linked to the aircraft in terms of CTO/CTA. These time-constraints are achieved by minor speed adjustments to the aircraft speed profile. The intention is to adjust the speed for each pair of A/C in conflict during the 15 minutes time window in order to increase their separation to 7NM, which implies an additional 2NM uncertainty buffer at the conflict point.[15]

The efficiency of the ERASMUS tool was validated through fast-time simulations (FTS), where the TC-SA resulted into 80% reduction in the number of A/C potential conflicts handled by controllers, and allowing ATCOs to handle a 70% traffic increase without any increase in their current workload.[17]

Based on these results, SESAR decided to investigate this concept further, through the so-called Trajectory Adjustment through Constraint of Time (TRACT) service.[18] It is expected that TRACT will be developed to manage early (25 minutes look-ahead time) conflicts identification. Just like TC-SA function, TRACT assess expected conflicts within its look-ahead time and tries to resolve them by automatically issuing to the appropriate A/C, CTO constraints over the conflict point, achieved by minor speed adjustments in order to decrease the ATCO workload due to conflict assessment and monitoring.

It was concluded that a TRACT solution is only possible to conflicts involving i4D-capable aircraft and thus, it is well known that several enablers for TRACT are not available yet. [19] For this reason, TRACT is now being studied along with other automated support tools for conflict detection and resolution. [19] All these tools will provide services with different look-ahead times. However, they all lead to the same ultimate objective of eventually reducing the complexity of traffic in order to reduce controller's workload and increase capacity.

The above-discussed tools are automated tools providing strategic detection and resolution of 4D trajectory conflicts at execution/in-flight phase. They are said to provide

strategic detection of conflicts because they can detect conflicts at a longer look-ahead time horizon than a typical detection look-ahead used by the controllers.

In this paper, the method proposed is applicable at pre-flight DCB timeframe, and is considered as a dynamic DCB /Short-Term ATFCM Measures (STAM) as discussed later in the paper.

2 ATM nodes, links and junctions' topology

ATM operational network can be seen topologically as a set of fixed nodes (internal or external), directed links among nodes and links intersections (see **Figure 1**). Each internal node (i, j...) is, simultaneously, the sink and source points of traffic flow and they are representing the physical volume of airspace occupied by a Terminal Manoeuvring Area (TMA). The external nodes (k, l...) are also considered as sinks and sources of the traffic, but they are representing entry/exit points of the airspace under consideration.

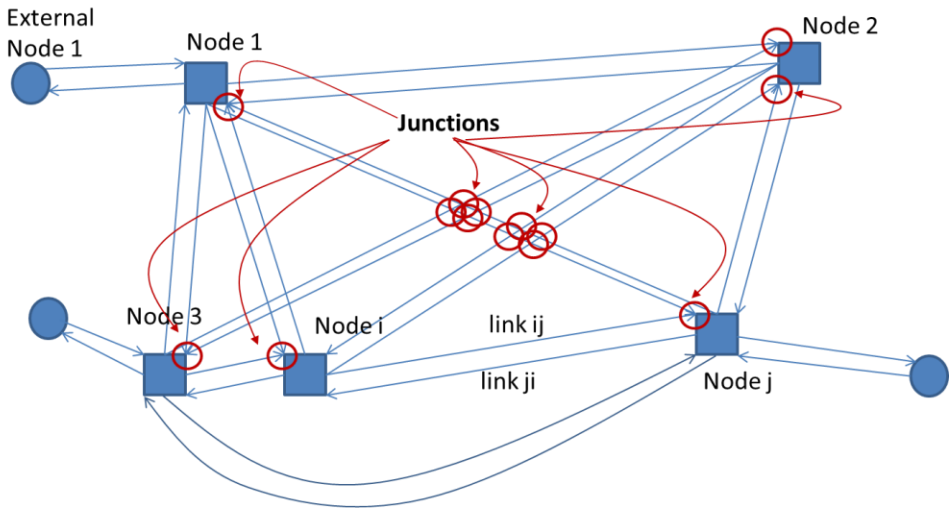

Figure 1.Airspace topology

An internal node (i), shown in **Figure 1** as a small square, has outbound traffics represented by exit links (from i to j) departing from any centre of each square's side, and inbound traffics (from j to i) represented entering by any square's corner. The external nodes are shown as circles, which also have outbound and inbound traffics, as shown in **Figure 1**.

Links represent planned A/C trajectory tracks, where the (unidimensional) continuity principle will be applied along them if they do not arrive to any junction. Finally, junctions are dynamic or fixed locations where two or more links are expected to converge. An intersection of links will only be considered as a junction if it is "active", that is; when a set of two or more A/C are expected to arrive within a small and well-defined time interval limit among any pair of them. These junctions might or might not be co-located with waypoints (WPs). In this research, WPs are classified in two different types: first, as airspace 3D points where some changes on the velocity vector are expected or, second, points set when a new operational condition applies.

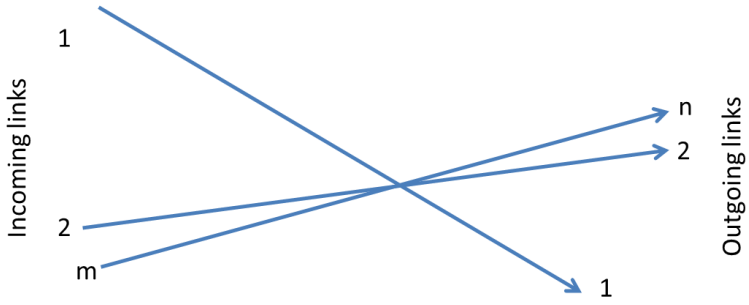

Figure 1. Junction geometries

In general, the geometry of a junction[20] can be defined by their physical intersection. The junctions could have *m* incoming links and *n* outgoing links (see **Figure 2**). When *n=m*, it is considered a crossing point whilst when *m>n*, it is named as a merging point. The nodes of the Air Traffic Service (ATS) route network are usually merging points**.** Finally, when *n<m*, the point is referred to as a distribution or a fork junction.

In this paper, it is assumed that outbound traffic (all flows emerging from node i towards all other nodes j, q_{ij}) and inbound traffic (all flows arriving from all nodes j coming to node i, q_{ji}) satisfies the limiting throughput criteria (QI_i) and (QO_i). Thus, considering all nodes (N), the following equations can be stated for each node (i):

$$QI_i \geq \sum_{j=1, j\neq i}^{N-1} q_{ji}$$

$$QO_i \geq \sum_{j=1, j\neq i}^{N-1} q_{ij} \quad (1)$$

Where, QI_i and QO_i are a priori known, possibly time dependant, maximum allowed flow values for each node (i).

Managing the TMA capacities in terms of inbound and outbound maximum flows (QI_i and QO_i) supported by E-AMAN/DMAN is considered as boundary conditions of the problem. For ATFCM purposes, all the required information from these nodes is provided for the above criteria. In other words, all the following discussion refers to airspace beyond the limits of the TMAs borders.

The first equation in Equation (1) also applies to the (active) junctions. That is to say; the whole maximum arriving traffic to the junction (m) shall be equal or smaller than the junction inbound flow capacity (QI_m). This capacity limit is particularly important at merging points (as when they are the entry points at the nodes), where the incoming traffic is confined into higher density outbound routes. The required "time to arrival change" raises very fast (towards infinite) when inbound traffic reaches the inbound flow capacity (QI_m).

As it is discussed later in this paper, an inbound flow capacity is very sensitive to TOA uncertainties. This condition implies that when confining air traffic in a fixed conventional ATS route network and maintaining the current levels of A/C TOA uncertainties, the proposed new ATFCM mechanism becomes unrealistic. Then, this paper postulates that most of the A/C are flying following free routing (FR) airspace. Free-routing airspace (FRA) enables direct trajectories and the RBT will improve their predictability.[14,21] In fact, flight plans will be more distributed over the entire airspace and then the traffic density will be generally more homogenously distributed (except those in the nodes entry points), then the expected probability of ATC interventions would be smaller. Therefore, the number of junctions will be higher and the average number of conflicts per junction will be reduced. This also implies that the ATCO's activities will shift from a situation of attending to a high number of conflicts, concentrated in specific junctions, to managing less conflicts per junction distributed over a much larger portion of the airspace.

As discussed later in this paper, when the inbound conflicted traffic exceeds the junction's inbound flow capacity (QI_m) established to be 6A/C per hour , the required

"TOA/Speed changes" to remove conflicts at junction becomes significantly high and may not be realisable by the A/C. To achieve realistic speed changes compatible with aircraft performance,[22] it is then postulated that most of the A/C are flying following free routing airspace (FRA), then the average traffic density per junction (except those in the nodes entry points) is low. For crossing point junctions within this context, the normal situation will then have an actual traffic flow below its limit. Under these circumstances, the situation can be dealt with as a traffic de-randomization problem (by speeding up and slowing down arriving traffic) to achieve a minimum "safe" time interval among all A/C arriving at the junction.

3 Conflict and hot spot strategic characterisation

Hot spots or A/C clustering consists in identifying groups of closely spaced A/C expected to arrive at a junction. The clustering process isolates a set of A/C that will be involved in multiple conflicts, close in time of arrival at a junction, ensuring that solving conflicts within each cluster separately, will not generate any new inter-cluster conflicts.[23] Cluster identification can be performed by using traffic complexity metrics, [20] or by aggregating space and temporal induced effects to all pairwise conflicts. In this paper, the latter criterion is used, determining the conflicts based on their expected TOA separation at the junctions, complemented with a spatial indicator regarding the traffic complexity for the conflict's surrounding area.

The method proposed in this paper is dealing with short-term ATFCM measure (STAM) issued short time before departure, during the pre-flight DCB timeframe, by including time constraints specifications into the initial RBT, or extended flight plan

(EFPL), to strategically and pro-actively remove expected conflicts at the merging points (junctions). This is achieved by incorporating minor adjustments in A/C Time of Arrival (TOA) at conflicted junctions. The proposed method is then acting at pre-departure phase, where EFPL provides more accurate 4D flight profiles description. Then the minor A/C TOA adjustments at hotspots to resolve expected conflicts should enhance the overall process of traffic management.

A key pillar required for the implementation of the proposed method, is to consider the A/C trajectories as the basis for both, the planning and execution phases of the ATM. These A/C trajectories must be continuously managed during their whole life cycle, since shared as SBT until fully completed in block time.

To determine the required TOA adjustments (achieved by minor speed changes) for removal of expected conflicts at the junctions, this paper discusses about the effect of the different sources of uncertainty in A/C TOA at junctions assuming pre-flight planning layer phase, the STAM time window, where a given probability of ATC intervention in resolving conflicts at junctions is established. The proposed method is then considered as a dynamic DCB /Short-Term ATFCM Measure (STAM).

It can be considered as complementary to another STAM currently studied under the SESAR 2020 exploratory research project, named “Cooperative departures for a competitive ATM network service (PARTAKE)”. [26] PARTAKE project is focussing on improving the air traffic dynamic demand capacity balancing, using as a window of opportunity, the prompt identification of “hot spots” at network level and re-adjusting the estimated take-off times within the assigned nominal CTOT margins, and rearranging the

departing sequence of aircraft at the involved airports to remove those hotspots. The proposed method in this paper and PARTAKE project are then somehow complementary, that is, if the computed TOA adjustments at junctions require speed changes that are unrealistic, PARTAKE can help-by adjusting the A/C's estimated take-off times.

Pairwise foreseen conflicts can be identified either by computing the expected separation at their closest point of approach (CPA) or by determining their expected time separation at the junction. Any A/C following predefined flight plans, typically defined at strategic level, usually have relevant along track unpredicted deviations, leading to strong variations on CPA location and distances. On the contrary, any A/C that usually has a well-defined 2D (or even 3D position, leading to a well-established 2D or 3D junction) will have uncertainties on their TOA. Hence, a definition of planned "time interval" between arriving A/C at a junction has been chosen to identify and to mitigate foreseen conflicts.

When minor speed changes are introduced to the initial flight speed profiles in order to remove conflicts at junction, the same proximate percentage of A/C's TOA at that junction will be modified. For instance, for an A/C flying at 400 knots for a flight distance of 134NM, if a speed change between 5% to 10% is applied, the A/C's TOA at junction will be also modified by 5% to 10%, equivalent to one to two minutes for every 20 minutes of A/C flight time.

In this paper, every foreseen conflict at any junction among all A/C is identified at strategic level and the required optimised TOA changes at this junction are computed. A Simple random sequence is used to generate initial time separation interval (τ_0) between

any two consecutive aircraft at the junction before TOA/ speed changes are applied. This initial time separation interval (τ_0) defined in Equation (24) is generated within the range of [0-9] minutes following a uniform distribution. This range of [0-9] minutes implies that each aircraft will initially require ATC intervention since we established 9 minutes as the minimum required separation at junction to reduce ATC intervention as discussed later in the paper. In other words, τ_0 represents the expected time interval between consecutive arrivals at the junction according to their flight plans. The new speeds applied to achieve TOA changes may induce conflicts at other junctions of involved A/C trajectories. Therefore, removal of a particular conflict demands an analysis of the whole set of junctions along the whole set of involved trajectories to take into account this interaction.

Additionally, at each crossing/merging point where the expected A/C TOAs have been changed, an analysis of complexity in the surrounding traffic should be performed by considering the A/C density and their intrinsic complexity, derived from a metric based on the ratios between their estimated velocities and distances to the junction.

Based on the two (temporal and spatial) criteria described above, for each (active) junction it is determined in this paper: First, whether the involved A/C have temporal (along their trajectories) impact (inducing other conflicts) over other intersected trajectories, and second; the complexity of the surrounding traffic is determined.

Figure 3 describes the twofold visions of conflict resolution impact: The vision on impact from along trajectories induced conflict and the vision on the complexity of the surrounding area.

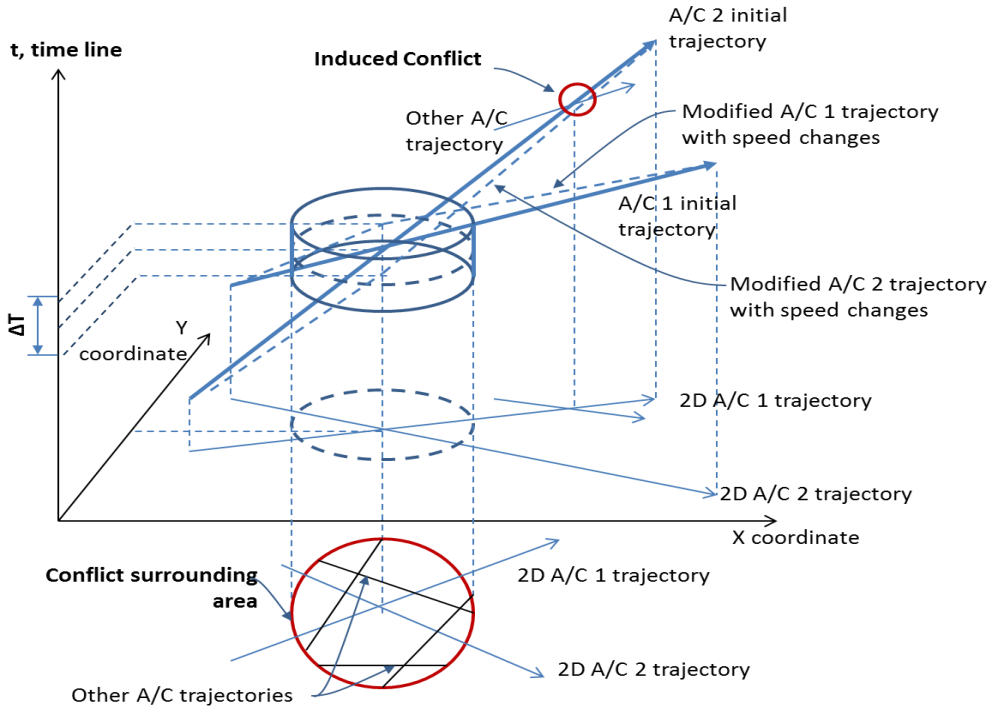

Figure 2. Spatial and temporal impacts for A/C conflict resolution.

4 Approach

4.1 Encounter removal for subliminal TOA changes based on speed control

At flow and capacity management level, the speed changes should minimise the expected probability of ATC intervention, providing estimated conflict free flight plans, but some additional criteria should be added to provide information about the characteristics of the perturbed area (referred in the **Figure 3** as conflict surrounding area).

The probability of 10^{-5} is set as the targeted probability for ATC intervention in resolving potential conflicts at any junction, obtained considering all uncertainties in the flight plan, as described in the RBT. This probability is derived from the total uncertainty in the A/C time of arrival (TOA) at junction and the resulting required minimum safe time interval between any two consecutive aircraft. It is discussed later in this paper that

for the derived total expected standard deviation ($\sigma_T = 1.5\ min$) in the TOA at junction, and to achieve an expected probability of ATC tactical intervention of 10^{-5}, it requires a minimum safe time interval ($\tau_p = 9$ minutes) between the expected TOA for any two consecutive A/C. Therefore, 9minutes interval is used in this paper as the required minimum time interval at the junction, when issuing time constrains in the RBTs.

For the proposed approach, incompatibilities of trajectories interdependencies are determined at strategic level, when issuing the RBT, as proposed in TBO, based on a given probability of ATC interventions.

The correlation between the geometry of links at junctions and ATCO workload has been previously acknowledged.[24,25] Indeed, understanding this geometry for foreseen conflicts is crucial in determining the most suitable technique (departing time, heading/2D-offset, and flight level and speed changes) to resolve it. Therefore, this paper recognises that subliminal time changes by speed control could not always be the distinctive technique to solve certain potential conflict geometries, demanding the concurrency of the others to cope with, at different stages of the flight plan's lifecycle.

For each (active) junction, the following parameters are relevant to characterise a conflict:

1. The time interval among the expected TOA of all A/C and their associated uncertainties;
2. The A/C navigation performance within the links;
3. The angle between the A/C trajectories centerlines at the junction;
4. The expected groundspeed for each A/C;

5. The expected relative altitude of each A/C before and after the crossing point.

Minor speed control technique to remove potential conflicts, shall consider these different encounter geometries.

4.2 Modelling approach

Recently, new classes of modelling approach in ATFCM based on either Lagrangian or Eulerian dynamics have arisen.[26,27] Lagrangian ATFCM models consider the dynamics of individual A/C; they can therefore, be seen as trajectory-based models. On the contrary, Eulerian models usually are macroscopic in nature. They are aggregated models, which consider the flow rates and densities in control volumes but do not track individual A/C trajectories.[27]

For Lagrangian models in ATFCM, the dimension of the problem grows proportionally with the number of A/C considered, and each individual trajectory must be precisely propagated in the network. Hence, Lagrangian models in ATFCM involving large numbers of A/C are generally computationally intensive.[26,27] Eulerian models on the other hand, focus on the aggregate properties of the air traffic network and hence, have lower fixed dimensions. As a trade-off however, the Eulerian models are generally not able to provide detailed information about each individual A/C.[27]

This paper provides a combined approach that, to some extent, uses both the Lagrangian and Eulerian views in a complementary manner. This approach allows an Eulerian aggregate optimal traffic flow to analyse local areas and Lagrangian knowledge of individual flight trajectories. The geometric characterisation of junctions is used for tracking the trajectory of each A/C to identify any conflicts and for providing required

speed changes of each A/C's trajectory. Each potential conflict among A/C is characterised by the time separation at their active junction. An aggregated local Eulerian vision is used as a metric to measure the complexity of the "disturbed" area where the conflict is located.

A time separation at the junction is used to formulate a cost function for conflict resolution, which relies on a linear programing solver that seeks to minimize the total A/C speed changes required for conflict resolution while maintaining their total flight time as a constraint.

In order to implement our conflict resolution model on realistic air traffic scenarios, we treat the required A/C separation by speed control as an optimization problem that has the following objectives:

1. Maximizing the total number of expected conflicts removed through subliminal speed changes;
2. Minimise the total amount of speed changes used for conflict resolution.

The minimum required time separation at a junction point is determined by considering the cross-track, along-track and scheduling uncertainties using a statistical method.

4.3 Linear programming optimisation problem for a pairwise crossing junction (n=m=2)

This section discusses a simple case where only two A/C and one crossing point are considered.

Figure 4 picturises the distance vs.time evolution to and from a crossing point of two A/C from their initial positions at points A and C respectively. Their initial trajectories are represented by solid lines, connecting to their next waypoints (B and D, respectively) after the crossing point. In this example, A/C from point C is being the second arriving A/C at the crossing point. The proposed speed changes involves slowing down the second arriving A/C (A/C at point C initially) up to the crossing point, and then flying above its nominal speed from this point. On the contrary, the first A/C arriving at the crossing point (A/C at point A initially) is doing the opposite. This approach provides a good platform to formulate the initial linear optimisation cost function to determine optimal speed changes for each A/C before and after the junction, subject to time constraints.

Two digit subscripts are used in **Figure 4**. The first digit subscript refers to situations before (denoted by 1) and after (denoted by 2) the junction. The second digit subscript refers to the involved A/C. Finally the tilde symbol (‘) refers to modified variables (speed or time) over the nominal ones (without tilde).

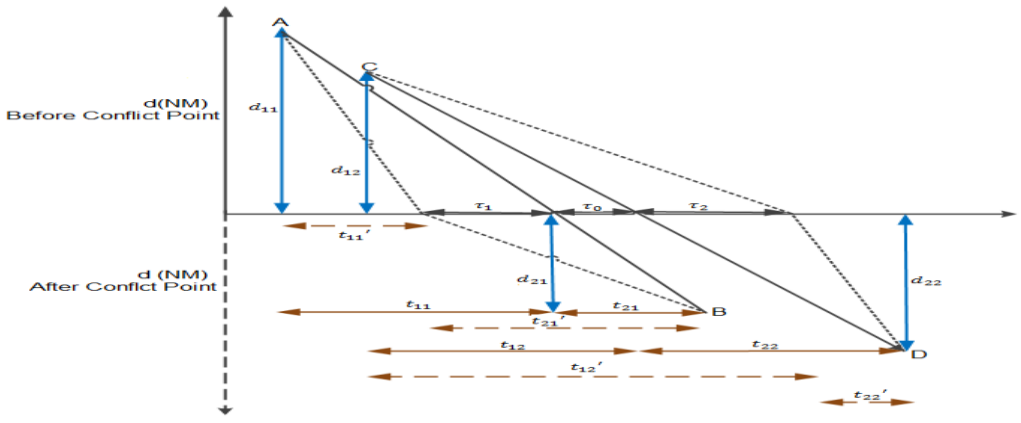

Figure 4.Distance /Time graph for A/C evolution to and from the junction

For the nominal and adjusted speeds (constant or average speeds are assumed) $V_{11} and\ V_{11}{}'$ of A/C1, the speeds are defined respectively as:

$$V_{11} = \frac{d_{11}}{t_{11}};\ V_{11}{}' = \frac{d_{11}}{t_{11}{}'}$$

The speed change can then be expressed as:

$$\Delta V_{11} = d_{11}\left(\frac{1}{t_{11}{}'} - \frac{1}{t_{11}}\right) \approx \frac{\tau_1 d_{11}}{t_{11}{}^2}$$
$$\Delta V_{11} = V_{11}\frac{\tau_1}{t_{11}}$$

Where τ_1 is the time in advance of the speeded up A/C arriving at the junction and let us call r_{11} its rate of time or speed change defined as:

$$r_{11} = \frac{\tau_1}{t_{11}}$$

That can be written as well as relative speed change:

$$r_{11} = \frac{\Delta V_{11}}{V_{11}} = \frac{\tau_1}{t_{11}} \quad (2)$$

Similarly from Figure 5, it can also be derived for the second A/C:

$$V_{12} = \frac{d_{12}}{t_{12}};\ V_{12}{}' = \frac{d_{12}}{t_{12}{}'}$$
$$\Delta V_{12} = d_{12}\left(\frac{1}{t_{12}{}'} - \frac{1}{t_{12}}\right) \approx -\frac{\tau_2 d_{12}}{t_{12}{}^2}$$
$$\Delta V_{12} = -V_{12}\frac{\tau_2}{t_{12}},$$

The ratio of time/speed change (r_{12}) is then:

$$r_{12} = -\frac{\Delta V_{12}}{V_{12}} = \frac{\tau_2}{t_{12}} \quad (3)$$

Following the similar processes, the required speed changes beyond the junction are obtained as follows:

For A/C 1:

$$\Delta V_{21} = -V_{21}\frac{\tau_1}{t_{21}},$$

$$r_{21} = -\frac{\Delta V_{21}}{V_{21}} = \frac{\tau_1}{t_{21}} \quad (4)$$

And for A/C 2:

$$\Delta V_{22} = V_{22}\frac{\tau_2}{t_{22}},$$

$$r_{22} = \frac{\Delta V_{22}}{V_{22}} = \frac{\tau_2}{t_{22}} \quad (5)$$

The postulated objective function (to be minimised) is then the aggregation of "ratios of change", weighed by their distances, that is:

$$J = [\, r_{11}d_{11} + r_{12}d_{12} + r_{21}d_{21} + r_{22}d_{22}] \quad (6)$$

And they are subjected to the following constraints:

$$\tau_1 + \tau_2 = \tau \text{ , achieving final aditional required time separation } (\tau) \quad (7)$$

$$r_{11}, r_{12}, r_{21}, r_{22} \leq 0.0X, \text{speed changes below } X\% \quad (8)$$

$$\frac{d_{11}}{(1+r_{11})V_1} + \frac{d_{21}}{(1-r_{21})V_1} = t_{11} + t_{21} \rightarrow t_{21}r_{11} - t_{11}r_{21} = 0, \text{unchanged total time } AC1 \quad (9)$$

$$t_{22}r_{12} - t_{12}r_{22} = 0, \text{unchanged total time AC2} \quad (10)$$

All the parameters required in the above optimization model are known except the minimum required time separation between the two A/C at the junction (τ). This parameter depends on the uncertainties of A/C's TOA and it is described later in this paper.

4.4 Example 1: elemental conflict removal by applying TOA subliminal changes

This example considers a basic scenario where the above linear optimization model is used to compute the required optimised speed changes for each A/C before and

after the joint for a pairwise junction. An ideal condition of no wind is assumed. Only two flights flying following the great circle are considered: BA560 from Oslo to Lisbon (ENGM-LPPT) and TAP761 from Rome to London (LIRA-EGLL). The main characteristics of the analyzed initial flight plans are presented in **Table 1**:

Table 1. Main characteristics of the analyzed initial flights plans

Flight	A/C	Flight Distance (NM)	Cruise Speed(Knots)	Flight time (Hrs)
ENGM-LPPT(BA560)	A320	1537	453	3.4
LIRA-EGLL (TAP761)	A320	820	440	1.86

The simulation exercise is performed using ATC2K simulator software.[28] The software uses a simulated Control Working Position (CWP) as the Human Machine Interface (HMI) for controlling the air traffic. It also presents a Conflict and Risk Display (CARD) feature which displays a table containing all potential conflicts between A/C pairs. The CARD includes: The predicted CPA time, the identity of involved A/C and additional highlights of the route segments in conflict. The situation before applying speed changes is shown in the left picture of **Figure 5** whilst the same situation after applying TOA changes is shown in the right picture.

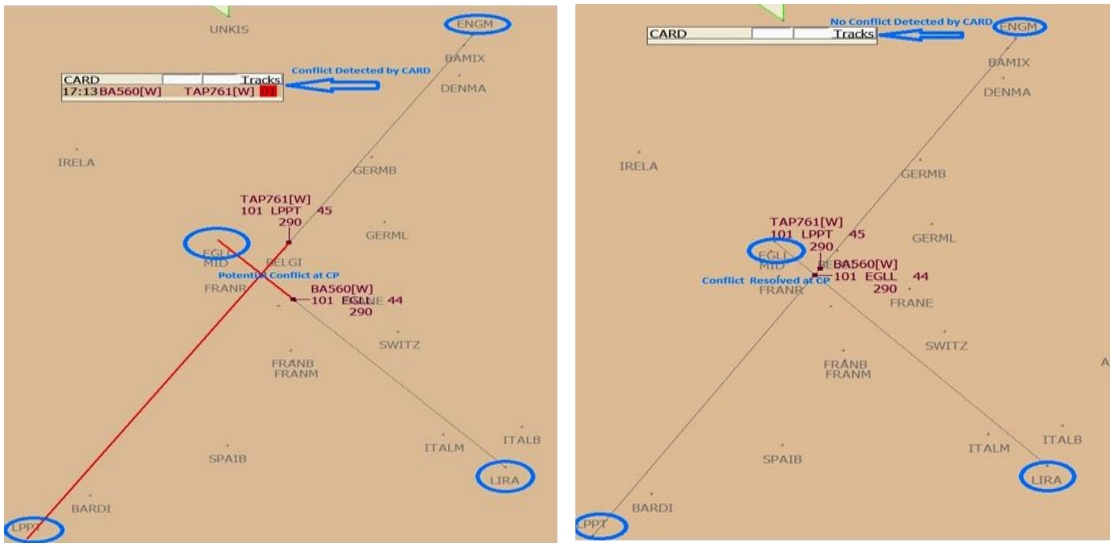

Figure 5.Conflict removal applying optimized TOA changes for 2A/C

In this example, applying the TOA changes is considered sufficient to resolve the conflict where speed changes ensure that the A/C TOA minimum interval is one minute. The outcomes of the linear optimization are summarized in **Table 2**:

Despite these promising results, the used strategic identification and removal of potential conflicts relies only on determinist assumptions and, therefore, conflict-free trajectories with respect to non-deterministic factors cannot be ensured. This is simply because the approach used in the example has omitted the characterisation of uncertainties and might have generated unrealistic solutions.

Table 2. The outcomes of the linear optimisation in Example 1

Flight	Speed change before junction	Speed change after junction
ENGM-LPPT(BA560)	$4kts$ (0.81%)	$1kts$ (0.25%)
LIRA-EGLL (TAP761)	$4kts$ (0.92%)	$0kts$ (0.04%)

4.5 Deriving the minimum required time separation at the junction (τ)

Pairwise conflicts are usually identified by computing their expected separation at their closest point of approach (CPA), even when the involved aircraft don't have a common shared point in their expected trajectories. When their trajectories share a common 3D point in their expected trajectories, the time of arrival's interval at the junction can also be used. Any A/C following a predefined flight plan, as defined in their RBT, usually have relevant along track unpredicted deviations, leading to strong variations on the location and separation at their CPA, whereas the common 3D point remains unchanged. Hence, a definition of "time interval" between arriving A/C TOAs at a junction has been chosen to identify and to mitigate potential conflicts in this paper.

The minimum required "safe" time separation (τ) between A/C at the crossing point or junction, defined at strategic level, depends on the degree of the adherence of the actual to the planned trajectory. Eurocontrol[29] defines the planned trajectory as the most likely behaviour of a flight through an area of interest over medium and long term planning horizons. As suggested in the definition, this trajectory may suffer from various sources of uncertainties as it is calculated on the basis of assumptions of expected A/C behaviour and, meteorological and other conditions. These uncertainties involve vertical, lateral (cross-track) and longitudinal (along-track) deviations. These deviations are assumed here as statistically independent or uncoupled.

Additionally, the uncertainties (due to initial time or scheduling) also affect the A/C TOA at the crossing point. The following sections describe and quantify all different sources of these uncertainties.

4.5.1 Effect of cross track errors

In the PBN concept, the lateral or cross-track deviation from a nominal trajectory is due to the Total System Error (TSE). It causes deviations on the actual junction coordinates. To establish the contribution of these errors on the time separation deviations, **Figure 6** shows an example of two A/C; A/C j and A/Ci, each assumed flying in a straight trajectory.

The solid lines represent the trajectory centrelines whilst the doted lines represent the lateral deviations. The ideal trajectories for the A/C i and j can be expressed respectively by the following equations:

$$y = a_i \cdot x + b_i$$
$$y = a_j \cdot x + b_j$$

Since, at the intersection point, the two equations have the same coordinates, by equating the two equations and solving for x and y, then:

$$x = \frac{b_j - b_i}{a_i - a_j}$$

$$y = \frac{a_i b_j - a_j b_i}{a_i - a_j}$$

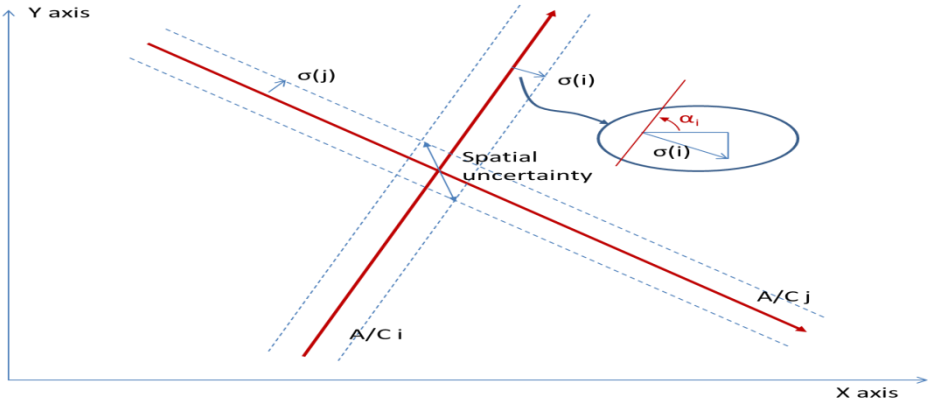

Figure 3.Geometrical uncertainties at the crossing point

It can be noted that the lateral deviations are due to changes in the value of coefficients b_i and b_j of trajectories equations (δb_i,δb_j), moving the junction coordinates (δx,δy) within an uncertainty area. The deviations due to these variations can be expressed in the following matrix form:

$$\begin{bmatrix}\delta x\\ \delta y\end{bmatrix} = \begin{bmatrix}\frac{-1}{a_i-a_j} & \frac{1}{a_i-a_j}\\ \frac{-a_j}{a_i-a_j} & \frac{a_i}{a_i-a_j}\end{bmatrix} \cdot \begin{bmatrix}\delta b_i\\ \delta b_j\end{bmatrix} \quad (11)$$

Based on this result, the covariance matrix for the junction coordinates error (δx,δy) can be derived from the (δb_i,δb_j) deviations. Multiplying matrix $\begin{bmatrix}\delta x\\ \delta y\end{bmatrix}$ in Equation (11) by its transpose matrix $[\delta x \quad \delta y]$ results in:

$$\begin{bmatrix}\delta x\\ \delta y\end{bmatrix} \cdot [\delta x \quad \delta y] = \begin{bmatrix}\frac{-1}{a_i-a_j} & \frac{1}{a_i-a_j}\\ \frac{-a_j}{a_i-a_j} & \frac{a_i}{a_i-a_j}\end{bmatrix} \cdot \begin{bmatrix}\delta b_i\\ \delta b_j\end{bmatrix} \cdot [\delta b_i \quad \delta b_j] \cdot \begin{bmatrix}\frac{-1}{a_i-a_j} & \frac{-a_j}{a_i-a_j}\\ \frac{1}{a_i-a_j} & \frac{a_i}{a_i-a_j}\end{bmatrix}$$

Which gives:

$$\begin{bmatrix}\delta x^2 & \delta x\delta y\\ \delta x\delta y & \delta y^2\end{bmatrix} = \frac{1}{(a_i-a_j)^2}\begin{bmatrix}-1 & 1\\ -a_j & a_i\end{bmatrix} \cdot \begin{bmatrix}{\delta b_i}^2 & \delta b_i\delta b_j\\ \delta b_i\delta b_j & {\delta b_j}^2\end{bmatrix} \cdot \begin{bmatrix}-1 & -a_j\\ 1 & a_i\end{bmatrix} \quad (12)$$

The covariance matrix is defined as the expectation for the above equation and becomes:

$$\begin{bmatrix}{\sigma_x}^2 & \sigma_{xy}\\ \sigma_{xy} & {\sigma_y}^2\end{bmatrix} = \frac{1}{(a_i-a_j)^2}\begin{bmatrix}-1 & 1\\ -a_j & a_i\end{bmatrix} \cdot \begin{bmatrix}{\sigma_{b_i}}^2 & 0\\ 0 & {\sigma_{b_j}}^2\end{bmatrix} \cdot \begin{bmatrix}-1 & -a_j\\ 1 & a_i\end{bmatrix} \quad (13)$$

Taking x-axis as coincident with the trajectory of the A/C i with $a_i = 0$ gives:

$$\sigma_{b_i} = \sigma_{LD_i} \quad (14)$$

$$\sigma_{b_j} = \frac{\sigma_{LD_j}}{\cos(\alpha_j)} \quad (15)$$

where α_j is the angle between trajectories.

The variance for the position uncertainty is derived from the trace of the covariance matrix (Equation (13)), such that the standard deviation for the position of the junction results into a function of the standard lateral deviation of trajectories (σ_{LD_i},σ_{LD_j}) assumed equals (σ_{LD}) and the angle between them (α_j) given by:

$$\sigma_{CP} = \frac{\sigma_{LD}}{\sin(\alpha_j)}\sqrt{2} \quad (16)$$

From **Figure 6**, the cross track uncertainty on the junction position obtained in terms of distance ($2\sigma_{CP}$), can be converted into a time standard deviation caused by this position deviation such that:

$$\sigma_{T1i} = \frac{\sigma_{CP}}{V_i} \quad (17)$$

$$\sigma_{T1j} = \frac{\sigma_{CP}}{V_j} \quad (18)$$

4.5.2 Vertical uncertainties

A Particular interest is required for those crossing points, where involved A/C are crossing their altitudes (or flight levels) around their 2D junction location. As it is well-known, vertical A/C evolution contains a broad range of sources of uncertainty variability, caused by atmosphere states, A/C performance/weight and efficiency criteria applied by the airline operator.

To cope with this situation, whilst maintaining a conservative approach, it is postulated in this paper that the involved A/C in this situation will be considered as if they were flying at the same altitude at the junction.

4.5.3 Initial time (Scheduling) uncertainty

Figure 7 shows the scheduling uncertainties, expressed as initial time errors. Considering their standard deviations, say σ_{T2i} and σ_{T2j}, these values are translated directly with the same values to the crossing point.

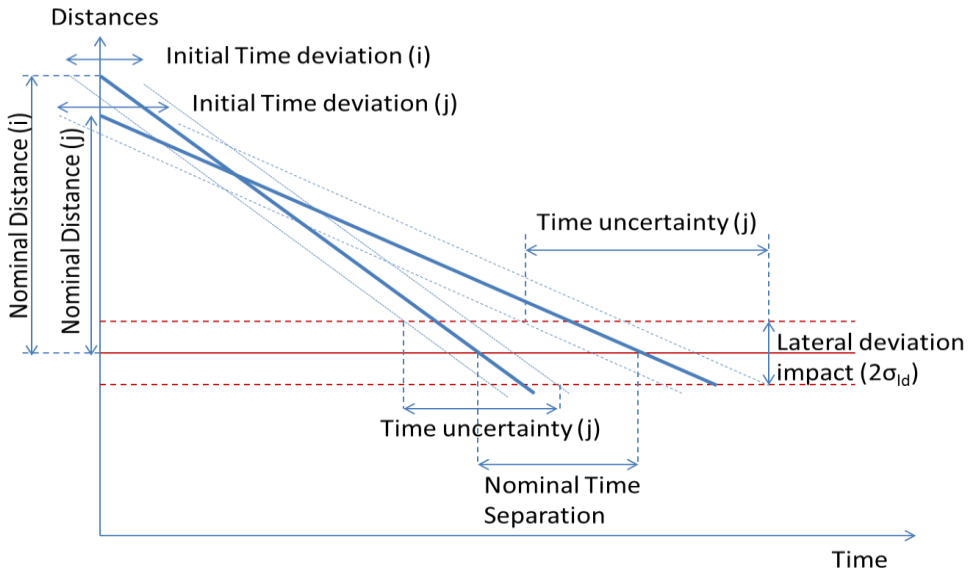

Figure 4.Translation of lateral deviations to time deviations at CPA

4.5.4 Along-track time uncertainties at the crossing point

The along-track uncertainty is due to the actual ground speed being different from the expected speed (V_0). This along-track error drifts linearly with time. In order to derive the impact of a long-track time errors, it is assumed in this paper that the distance (d) to the crossing point is known. Then, the expected flight time (t_0) to this point is given by:

$$t_0 = \frac{d}{V_0}$$

Any deviation (δV) in the ground speed (V_0) will involve a change in the arrival time, given by:

$$\delta t = -\frac{d \cdot \delta V}{V^2} \approx -\frac{d \cdot \delta V}{{V_0}^2} \quad (19)$$

From this result, the standard deviation σ_{T3} for the TOA (δt) to the junction, due to errors into the ground speed, having standard deviation of σ_v, can be directly obtained:

$$\sigma_{3T} = \frac{d}{{V_0}^2} \cdot \sigma_V \quad (20)$$

In summary, A/C i and j trajectory lateral deviations, initial time and along-track time deviations are transferred as time uncertainties to the junction with values for their standard deviations shown in **Table 3**

Table 3. Summary of sources of uncertainties expressed as standard deviations

Uncertainty at the junction	A/C I, j TOA standard deviation
Due to A/C lateral deviation ($\sigma_{T1i,j}$)	$\sigma_{T1i,j} = \sqrt{2} \cdot \frac{\sigma_{LD}}{V_{i,j} \cdot \sin(\alpha_{ij})}$
Due to Initial time deviation ($\sigma_{T2i,j}$)	$\sigma_{T2i,j}$
Due to a long-track time deviation ($\sigma_{T3i,j}$)	$\sigma_{T3i,j} = \frac{d_{i,j}}{{V_{i,j}}^2} \cdot \sigma_{Vi,j}$

4.5.5 Criteria for pairwise time separation at the junction

Based on previous discussion, considering those three sources of errors being statistically independent and assuming Gaussian distribution applied to all of them, the required time interval (τ) can be derived from a predefined expected probability of ATC intervention (P_c) at the junction .

The total standard deviation on the TOA can be computed for A/C i and j as:

$$\sigma_{Ti,j} = \sqrt{{\sigma_{T1i,j}}^2 + {\sigma_{T2i,j}}^2 + {\sigma_{T3i,j}}^2} \quad (21)$$

The expected probability of ATC intervention (P_c) can be computed by convolving the two associated probability density functions (pdf) for A/C (i, j) for the time of arrival (t) to the junction for each of them given by:

$$f_i(t) = \frac{1}{\sqrt{2\pi\sigma_{Ti}}} e^{-\frac{(t-t_i)^2}{2\sigma_{Ti}{}^2}} \text{ , and } \quad f_j(t) = \frac{1}{\sqrt{2\pi\sigma_{Tj}}} e^{-\frac{(t-t_j)^2}{2\sigma_{Tj}{}^2}}$$

This convolution for both pdfs gives the probability of A/C i, j arriving at the same time:

$$P_C = \frac{1}{\sqrt{2\pi(\sigma_{Ti}{}^2+\sigma_{Tj}{}^2)}} e^{-\frac{(t_i-t_j)^2}{2(\sigma_{Ti}{}^2+\sigma_{Tj}{}^2)}} = \frac{1}{\sqrt{2\pi(\sigma_{Ti}{}^2+\sigma_{Tj}{}^2)}} e^{-\frac{\tau_p{}^2}{2(\sigma_{Ti}{}^2+\sigma_{Tj}{}^2)}} \quad (22)$$

The required time interval (τ_p) between their expected TOA for a given P_c then results in:

$$\tau_p = \sqrt{-2\left(\sigma_{Ti}{}^2 + \sigma_{Tj}{}^2\right) Ln[P_C \cdot \sqrt{2\pi(\sigma_{Ti}{}^2 + \sigma_{Tj}{}^2)}]} \quad (23)$$

If the expected (nominal) time interval (τ_0) is equal or greater than the above computed value (τ_p), there will be no additional time interval required. Otherwise, the demanded time increment shall be:

$$\tau = \tau_p - \tau_0 \quad (24)$$

4.6 Junction inbound capacity and TOA uncertainties

Figure 8 Shows the required TOA interval (τ_p) for different global standard deviations $(\sqrt{(\sigma_{Ti}{}^2 + \sigma_{Tj}{}^2)})$ in the TOAs for A/C i and j at the junction with different chosen expected probability of ATC intervention (Pc).

By assuming a constant TOA interval (τ_p) between consecutive A/C, the maximum inbound flow at the junction (the frequency of traffic) can be directly derived as:$QI_m = 1/\tau_p$. It can be derived from **Figure 8** that in order to maintain expected probability of ATC intervention below 10^{-3} and a junction capacity close to 6 A/C per hour, a global TOA uncertainty of 3 minutes or less will be required.

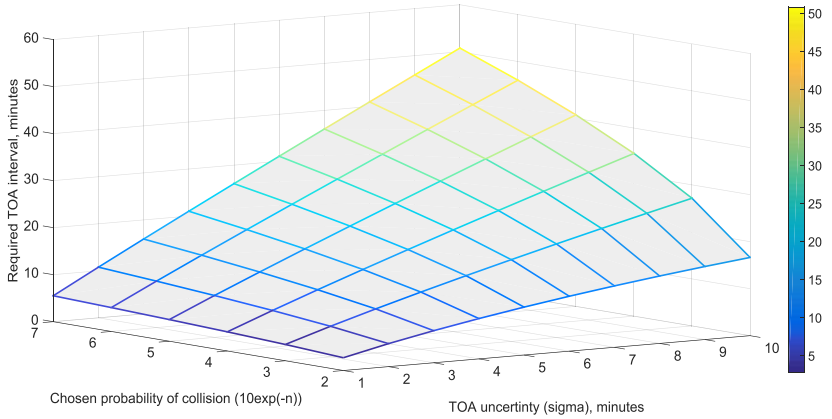

Figure 8.Required TOA interval for different collision probabilities and TOA standard deviation for the involved A/C

The results above quantitatively indicate the strong sensibility of the required TOA interval to the A/C TOA uncertainties. This also concludes that the proposed planned strategic changes for these TOAs allow a maximum rate of up to 6 A/C of inbound traffic flow per hour only when the actual A/C TOA uncertainty is reduced below 3 minutes of the standard deviation.

As discussed below, however, this TOA standard deviation value can only be achieved under specific operational and A/C capabilities conditions.

Uncertainties due to lateral deviations, given in terms of standard deviation ($\sigma_{T1i,j}$), as expressed in **Table 3**, depends on the navigation performance accuracy (given

by σ_{LD} or RNP), A/C ground speed ($V_{i,j}$), and angle between A/C trajectories/tracks (α_{ij}). This dependency is shown in **Figure 9**. As can be observed, for crossing angles $\alpha_{ij} \leq 20^0$ and speeds $V_{i,j} \leq 200kt$ the resulting relative TOA standard deviation is:

$$\sigma_{T1i,j}/\sigma_{LD} \geq 1min/NM.$$

Assuming for a typical commercial A/C with a speed greater than 200 knots and the crossing angle between tracks greater than 20^0 then, under these conditions, the relative TOA standard deviation is: $\sigma_{T1i,j}/\sigma_{LD} < 1min/NM$.

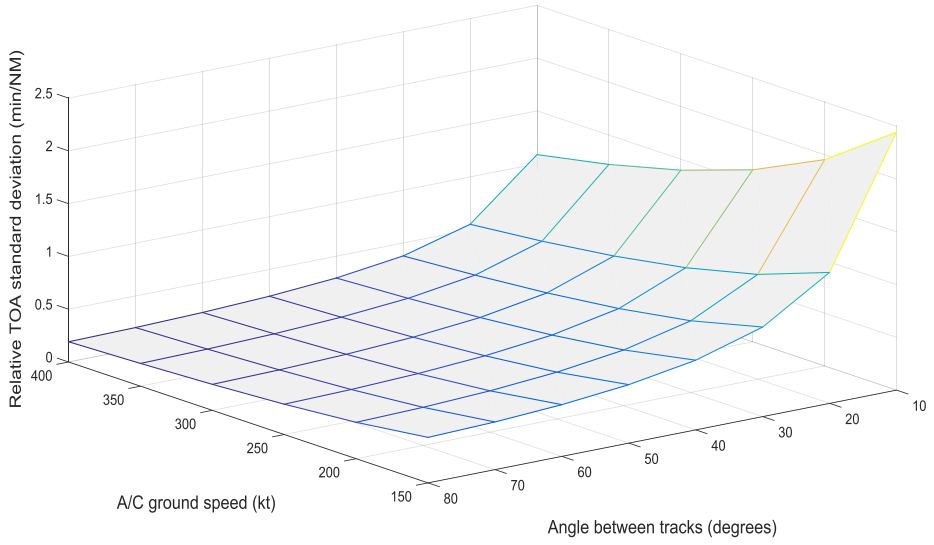

Figure 9.Resulting relative TOA standard deviation vs. A/C speed and tracks crossing angle

The accuracy criteria for RNP-X involves a standard deviation of $\sigma_{LD} = X/2$. This means that when an A/C is flying under PBN with RNP-X procedures, the associated standard deviation is $(X/2)$. For instance, RNP1 involves a standard deviation of $\sigma_{LD} = 0.5NM$. This then results in TOA standard deviation; $\sigma_{T1i,j} < \frac{\sigma_{LD}1min}{NM} = 30s$.

Concerning the initial/scheduling time deviations ($\sigma_{T2i,j}$), this variable can hardly be known a-priori, especially due to the limited runway capacities constraining departures. According to the Eurocontrol PRR 2014,[30] 0.9 minutes per departure due to local ATC departure delays at the gate and 3.5 minutes delay per departure due to additional taxi-out time were registered at the top 30 busy airports in Europe in 2014. These delays can be reduced by applying new operational concepts such as A-CDM[31] at the airport by synchronising activities of all involved players to maximise the departure predictability. Other ongoing research projects such as the UDDP[31] seeks to significantly reduce the level of these inefficiency to a target of about 30 seconds.[31] Although the previous average values sensitivities are not known, in this paper, an initial/scheduling time standard deviation of around 1 minute ($\sigma_{T2i,j} = \pm 1$ minute) has been adopted.

The last source of uncertainty is the along track deviation ($\sigma_{T3i,j}$). This depends on the A/C ground speed errors (expressed by $\sigma_{Vi,j}$), the distance flown ($d_{i,j}$) and the A/C ground speed ($V_{i,j}$). 12 kts has been often used as a typical standard deviation for ground speed errors,[32] with this value, **Figure 10** shows the impact of A/C nominal ground speed ($V_{i,j}$) and the distance to junction ($d_{i,j}$) on the along track deviation ($\sigma_{T3i,j}$).

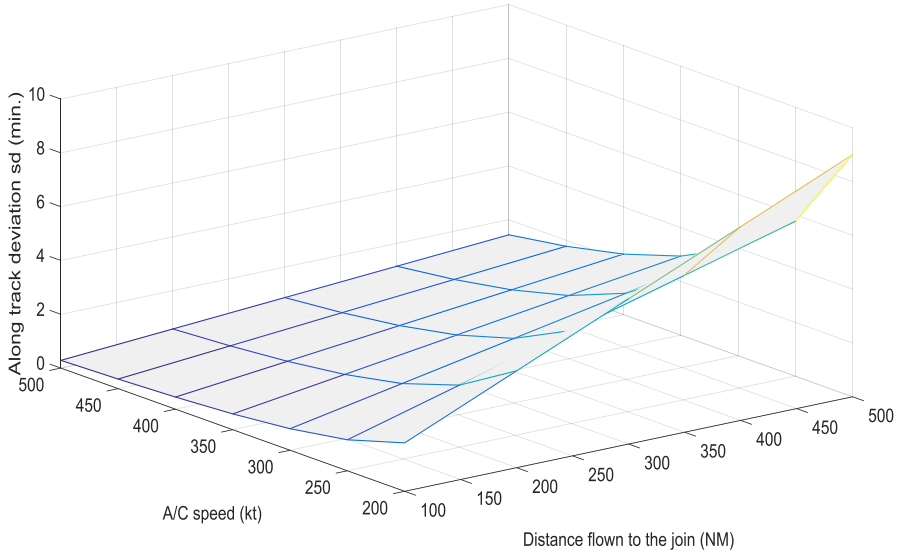

Figure 10.Resulting along track standard deviation vs. A/C speed and distance to the junction for 12 knots of ground speed uncertainty standard deviation

When the distance flown to the junction is above 500NM, the along track standard deviation grows above two minutes for A/C's speeds below 400 knots. These results clearly show that along track deviations reach an unacceptable level of uncertainty for many practical flight plans, reducing the junction's "safe" capacity to below reasonable operational level.

To overcome these problems, it is assumed that the A/C are equipped with an on-board CTA functionality with the accuracy of ± 30 seconds. It has been suggested that the use of this CTA accuracy value is more effective for dynamic Demand & Capacity Balancing than that of TTO/TTA accuracy (±3 minutes).[32] However, even relaxing the CTA accuracy ($\sigma_{T3i,j} = \pm$ 30 seconds) to $\sigma_{T3i,j} = \pm 1$ minute, an acceptable result can be achieved.

In summary, it has been pointed out how a junction inbound flow capacity strongly depends on TOA uncertainties (**Figure 8**). Only when these are below a few minutes, the expected flow capacity level remains enough to support the proposed application of subliminal changes on the planned A/C TOA to the junctions. **Table 4** specifies the adopted values of requested TOA standard deviation, based on the assumptions made above.

The resulting final combined TOA standard deviation ($\sigma_T = 1.5$ minutes) is used to re-establish the required TOA interval for different collision probabilities. For these TOA standard deviations, the minimum time interval between consecutive A/C, derived from Equation (23), is presented in **Figure 11** for different probabilities of collision (P_C).

Table 4. Summary of assumed Required TOA standard deviations

Uncertainty at the junction	A/C TOA standard deviation specification	Required condition
A/C lateral deviation	$\sigma_{T1i,j} = 30s$	Crossing angle $\alpha \geq 20^0$ and RNP1
Initial time deviation	$\sigma_{T2i,j} = 1min$	-
Along-track time deviation	$\sigma_{T3i,j} = 1min$	A/C CTA equipped
Combined time deviation	$\sigma_T = 1.5min$	All of the above

As shown in **Figure 11**, the expected probability of ATC intervention of 10^{-5} requires a minimum time interval of around 9 minutes, which permits the junction's inbound traffic flow of up to 6A/C an hour. This value for the collision risk is then

retained, by considering it will strongly reduce the probability of ATC tactical intervention to remove conflicts.

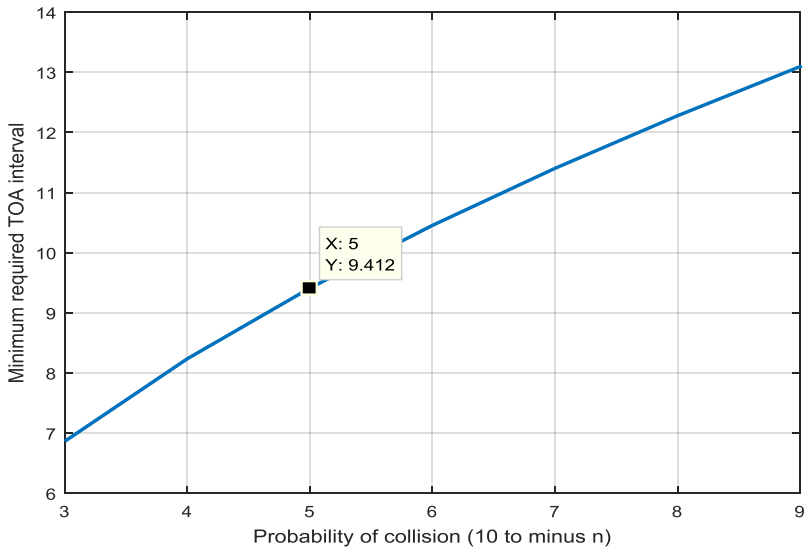

Figure 11.TOA interval for different probabilities of collision at the junction

4.7 Criteria for A/C time separation at the junctions along trajectories

So far, our discussion has considered a single crossing point of pairwise separation problem. In this section, the problem with multiple junctions along the trajectory is discussed.

Any link, which represents an A/C planned trajectory (i) can have different junctions where some TOA changes are required. Additionally, more than two A/C might demand changes in their expected arrival times at the same junction. **Figure 12** shows the distance/time evolution for A/C (i) having two consecutive junctions ($m, m+1$) where changes in the expected TOA are required for A/C i and j at junction m, and for A/C i, k and l at junction $m+1$.

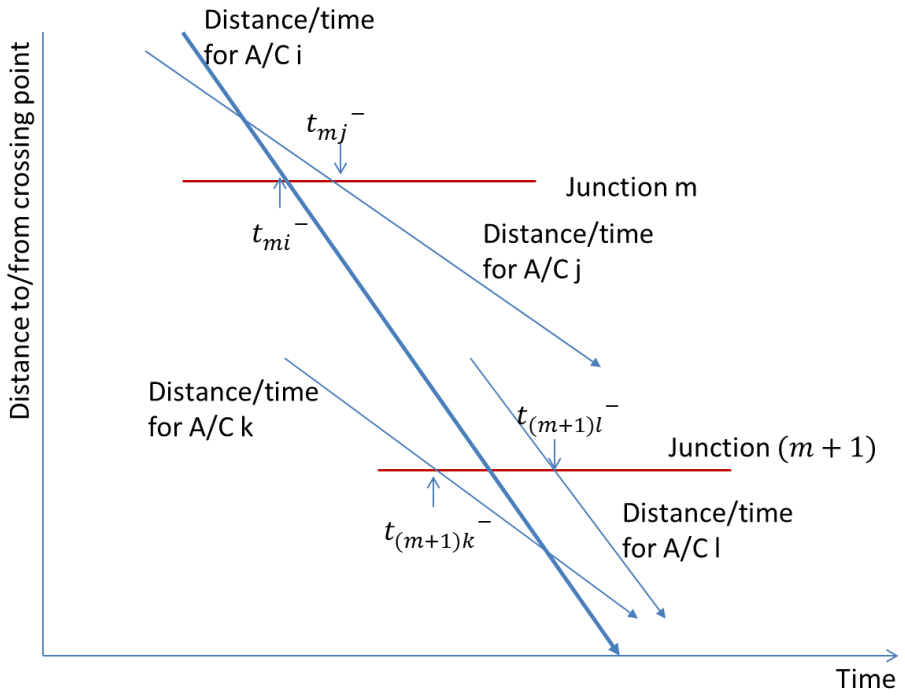

Figure 12.Distance/time evolution for A/C i, having conflicts at nodes m and n

To maintain the global time performance, a set of new TOA ($t^{+}{}_{mi}$) at each junction is chosen to have the same mean time (t_{m0}) as the one for the times before applying speed changes ($t^{-}{}_{mi}$), that is to say:

$$t_{m0} = \frac{\sum_i t^{-}{}_{mi}}{N_m} = \frac{\sum_i t^{+}{}_{mi}}{N_m} \quad (25)$$

The above closure condition assumes that the average traffic flowing at this junction is low enough to allow finite time changes ($t^{+}{}_{mi}$).

For any junction (m), the "junction equation" derived below provides the new TOA. In this problem definition, each A/C is assigned with a subscript with the number of the order they arrive to the junction (e.g., 1,2,..). The time interval (τ_{pq}) between any

two consecutive A/C (say, p and q) can be derived from Equations (23) and (24) with the following set of equations applied:

$t^+_{m2} - t^+_{m1} = \tau_{m21}$
$t^+_{m3} - t^+_{m2} = \tau_{m32}$
$t^+_{mn} - t^+_{m(n-1)} = \tau_{m(n-1)n}$
$t^+_{m1} + t^+_{m2} + .. t^+_{mn} = n \cdot t_{m0}$ (Closure condition)

These equations allow us to compute the new (n) TOA at junction (m). The above system has to be solved over "all (active) junctions in the network" that are demanding a new TOA.

Once all new times (t^+_{mi}) have been computed for each node (m) and for each involved A/C (i) (see **Figure 13**), the required speed changes can be easily established. Let's define the following variables and constants:

V_m^{m+1}; Speed between junctions m and $m+1$,

d_m^{m+1}; Distance between junctions m and $m+1$ (constant),

Δt_m^{m+1}; Time of travel between junctions m and $m+1$,

These variables are inter-related by the following equation:

$$V_m^{m+1} = \frac{d_m^{m+1}}{\Delta t_m^{m+1}} \quad (26)$$

Variations on the speed between junctions (V_m^{m+1}) are related to the variations on the travel time (Δt_m^{m+1}) by:

$$\delta V_m^{m+1} = -\frac{d_m^{m+1}}{(\Delta t_m^{m+1})^2} \delta(\Delta t_m^{m+1}) \quad (27)$$

Where the variations on the travel time ($\delta(\Delta t_m^n)$) are known and given by:

$$\delta(\Delta t_m^{m+1}) = (t^+{}_{m+1} - t^-{}_{m+1}) - (t^+{}_m - t^-{}_m) \quad (29)$$

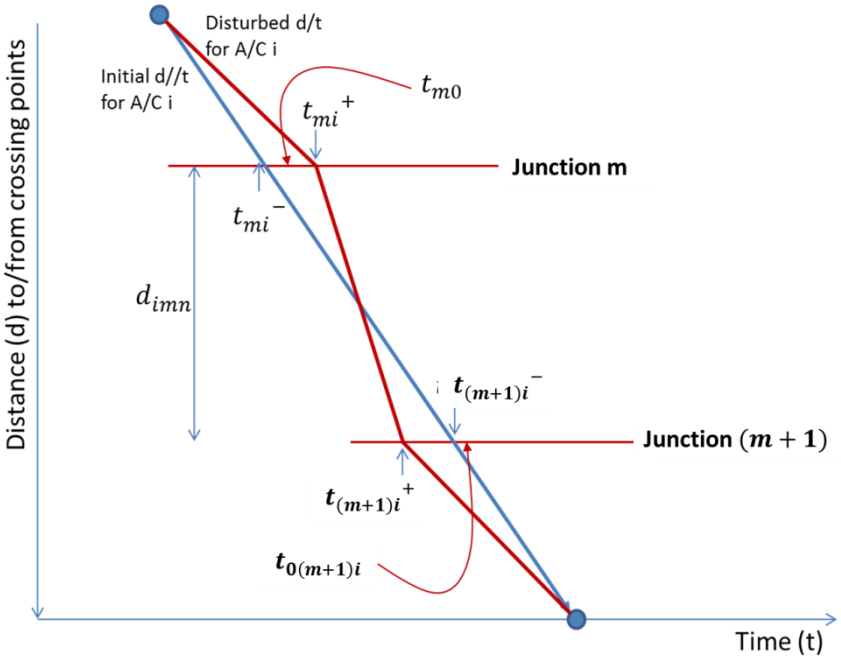

Figure 13.Nominal and perturbed distance/time evolution for A/C i

In other words, all the speed changes (δV_m^{m+1}) can be directly computed by applying the following equation to all trajectories (i) where some amount of speed change is required:

$$\delta V_{im}^{m+1} = -\frac{d_{im}^{m+1}}{(\Delta t_{im}^{m+1})^2}\left[\left(t^+{}_{i(m+1)} - t^-{}_{i(m+1)}\right) - (t^+{}_{im} - t^-{}_{im})\right] \quad (30)$$

4.8 Optimising the speed changes with multiple junctions

When the above closure condition (Equation (25)) was imposed, the amount of required speed changes demanded of the different involved A/C was ignored; this may lead to some unrealistic solutions. To overcome this risk, the closure condition is removed and replaced by a linear optimisation problem where the cost function

represents the global speed changes for the involved A/C population. From Equation 30, the speed change in segment (m to $m+1$) for flight (i) can be expressed as a function of the required time changes at both nodes:

$$\tau_{i(m+1)} = \left(t^{+}{}_{i(m+1)} - t^{-}{}_{i(m+1)}\right)$$
$$\tau_{im} = \left(t^{+}{}_{im} - t^{-}{}_{im}\right) \quad (31)$$

The longer the distance along which this speed change is applied, the worst flight efficiency will be for the involved A/C. Then the "cost" for this particular perturbation can be modelled by the product of: $\delta V_{im}^{m+1} \cdot d_{im}^{m+1}$, which leads to a global cost function obtained as sum of these elementary contributions given by:

$$J = \sum_i \sum_m \delta V_{im}^{m+1} \cdot d_{im}^{m+1} = -\sum_i \sum_m \left[\frac{d_{im}^{m+1}}{\Delta t_{im}^{m+1}}\right]^2 \left[\tau_{i(m+1)} - \tau_{im}\right] \quad (32)$$
$$= -\sum_i \sum_m [V_{im}^{m+1}]^2 \left[\tau_{i(m+1)} - \tau_{im}\right]$$

This cost function is subject to the following conditions:

At each junction, the n number of arriving A/C shall follow:

$$t^{+}{}_{m2} - t^{+}{}_{m1} \leq \tau_{m21}$$
$$t^{+}{}_{m3} - t^{+}{}_{m2} \leq \tau_{m32}$$
$$t^{+}{}_{mn} - t^{+}{}_{m(n-1)} \leq \tau_{m(n-1)n} \quad (33)$$

Furthermore, all relative speed changes (δV_{im}^{m+1}) shall be below a given maximum (X %). Additionally, the total flight time shall be maintained, then for the last junction or node (k) of each flight (i), the final arrival time shall be maintained. Therefore, for all affected A/C (i), the following conditions applies

$$\delta V_{im}^{m+1} \leq 0.0X \cdot V_{im}^{m+1} \qquad (34)$$
$$t^{+}_{ki} = t^{-}_{ki}$$

The above cost function with the associated constraints should provide an optimised set of proposed speed changes, removing all expected conflicts where the required TOA's changes are sufficiently small to maintain the total flight time by applying slight speed changes for all involved A/C.

4.9 Examples for merging conflict removal at single/multiple Junctions by applying TOA subliminal changes

Different scenarios based on the number of A/C involved in the conflict at the junction, flight distance to the junction, initial time separation interval between any two consecutive A/C at the junction (τ_0) and the number of junctions (single junction or multiple junctions) are considered in the examples below.

Equation (24) considers τ_0 as the time separation interval between any two consecutive A/C at the junction before the subliminal speed changes are applied. This variable represents the interdependency of time stamps on A/C trajectories or the A/C closeness at the junction inherently in the flight plans.

For each scenario, the expected probability of ATC intervention for any two consecutive A/C is set to10^{-5}, hence its resulting required minimum TOA interval (τ_p) will be 9.5 minutes. The optimization model is applied for each scenario to obtain the required subliminal TOA change for each A/C providing this expected probability of ATC intervention. The results are then verified using simulations in the ATC2K simulator software.

Example1: Single Merging Junction. Consider six merging A/C at a single junction. It should be recalled that this value (6 A/C/hour) has been determined as close to the maximum arriving rate to a junction to achieve an expected probability of ATC intervention of 10^{-5} , other words, minimum time interval (τ_p) of 9.5 minutes. In this simulation example, the optimal speed changes are calculated for each A/C before and after the junction in order to maintain the required TOA interval.

All A/C in this example fly with the same speed of V=450 knots for a flight distance of 900NM to the junction. The time separation interval between any two consecutive A/C (τ_0) value is allowed to randomly vary within different intervals where each interval represents a different initial time stamp interdependency of A/C trajectories at the junction before TOA changes are applied. For each τ_0 interval between A/C, a different scenario is generated.

Figure 14, shows box and whisker plots of the speed changes (in percentage of A/C speed) obtained by the optimisation model to remove merging conflict scenarios for τ_0 intervals changing randomly within the ranges [0-9], [0-8], [0-7], [0-6], [0-5] minutes and [0-4] minutes respectively, which represent scenarios above the throughput of the junction.

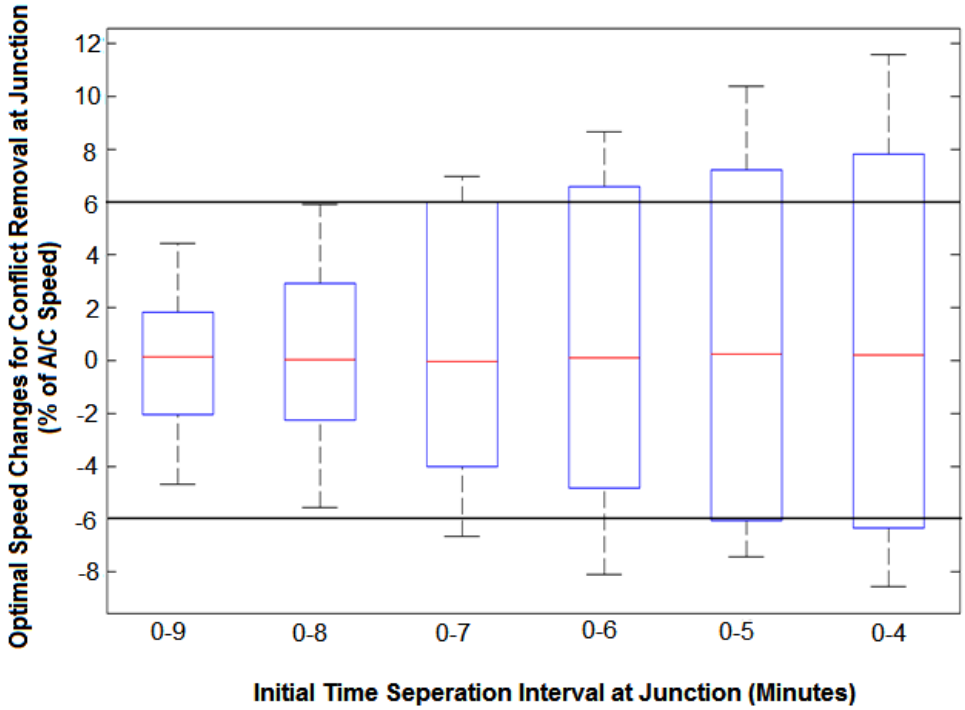

Figure 14.Statistics for the required speed changes at Junction for different randomized time separation intervals between consecutive A/C, for a set of 6A/C in bound a junction

As shown in **Figure 14**, for random τ_0 variations within intervals of [0 9] and [0 8] minutes, the obtained speed changes are all below 6%, for [0 7] minutes interval, still the 50^{th} percentile is under this threshold.

The conflict situation in **Figure 14** before and after TOA changes are applied is analysed through a series of simulations using ATC2K simulator, the results are shown in **Figure 15**. The left hand side shows the situation before, while its right hand side shows the situation after TOA changes are applied.

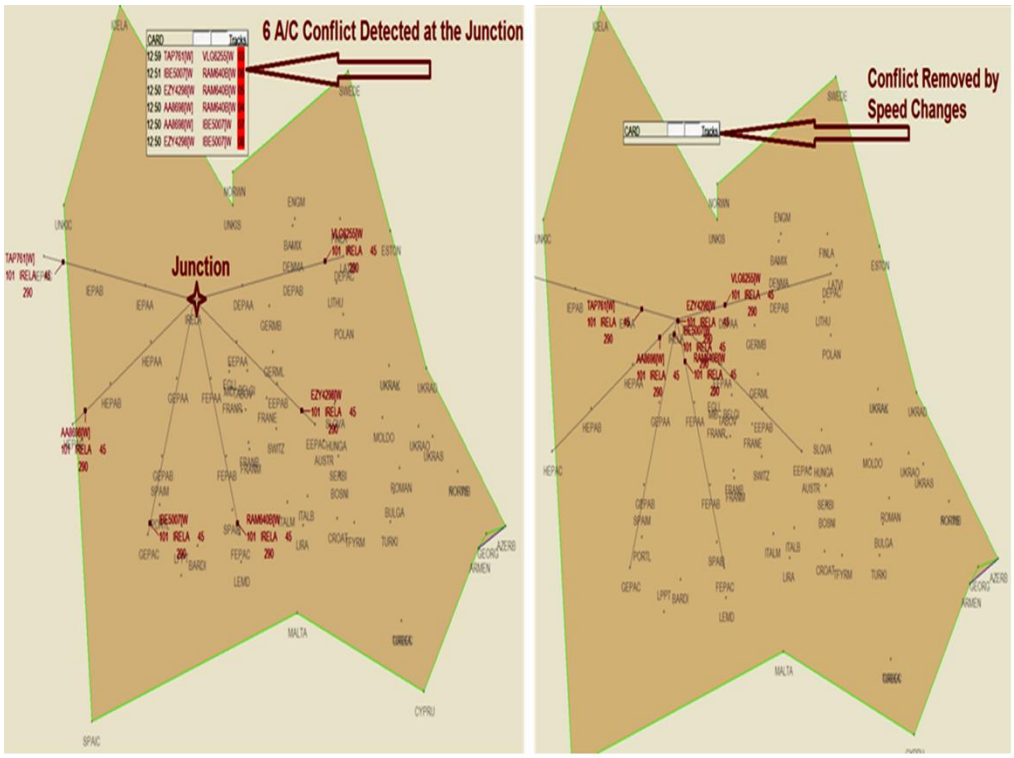

Figure 15.Conflict removal for 6A/C merging to the Junction

Example 2: Multiple Junctions. As previously discussed in this paper, A/C may be in conflict at multiple junctions along its flight. For example **Figure 16**, shows 8 flights where the A/C denoted as A/C4 is involved in a conflict with other five A/C at junction 'm' and also with other two A/C at junction 'n'.

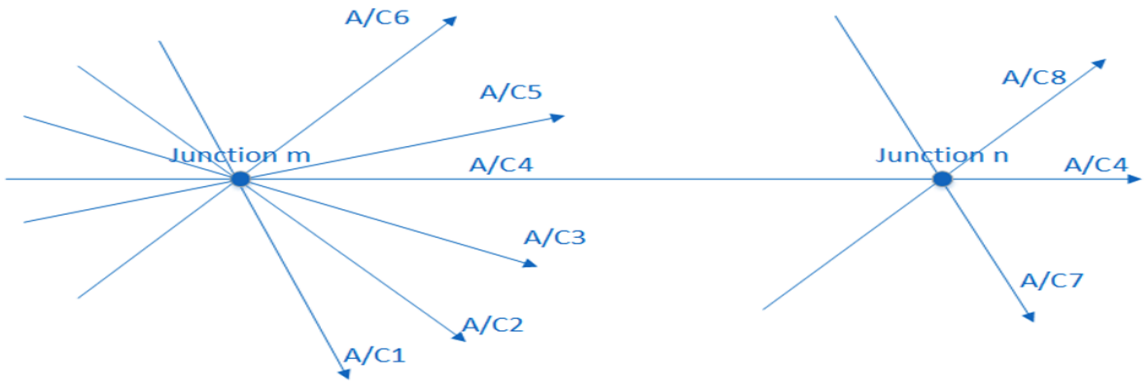

Figure 16.Conflict on multiple junctions involving 8A/C

Using the same traffic sample as used in the previous example but adding two A/C at the second junction, the optimisation model provides the required speed changes that resolve all the conflicts at both junctions providing the following results (see **Table 5**).

Table 5. Optimal speed changes for Multiple Junction Conflict Involving 8 A/C

τ_0 variation intervals(Minutes)		*8-9*	*7-9*	*6-9*	*5-9*	*4-9*	*3-9*
Optimal Speed Changes (% of A/C's Speed)	**A/C**			**First Joint**			
	A/C1	3.2731 -2.5738	4.5429 -3.5542	5.1760 -5.4552	8.9412 -8.2804	10.8340 -10.8359	13.1296 -13.3052
	A/C2	2.7878 -2.8995	5.3553 -5.4498	5.9990 -5.9438	7.6717 -7.1567	7.6493 -7.0368	9.6664 -8.3386
	A/C3	0.0574 -0.0694	2.3431 -2.7684	3.5855 -4.0640	2.3202 -2.4374	4.4268 -3.6789	1.9553 -2.9741
	A/C4	-1.4753 2.0553	-1.2932 1.7668	-0.2656 0.3484	-2.5493 4.2258	-1.9951 2.4911	-3.9895 4.5226
	A/C5	-2.1186 3.3740	-1.9689 3.0780	-4.9123 4.0083	-4.4023 7.4302	-5.2166 7.5429	-7.0531 9.6725
	A/C6	-2.1179 3.8212	-4.7596 5.2369	-6.1979 5.5880	-7.6655 8.9412	-9.7612 10.4107	-10.4172 13.5992
				Second Joint			
	A/C7	0.2088 -0.4149	0.6289 -1.2346	0.6289 -1.2346	0.6289 -1.2346	2.3454 -4.3825	0.2088 -0.4149
	A/C8	-0.5419 1.2658	-0.9138 2.1277	-1.6578 3.0961	-0.9138 2.1277	-0.9430 2.1277	-0.5419 1.2658
	A/C4	-1.8405	-1.4374	-1.4374	-1.7065	-0.7581	-3.9360

Figure 17 shows the statistics for the speed changes. It can be observed that speed changes are still below the 6% for randomised TOAs intervals between [0 9] and [0 8] minutes in this multiple junction situation.

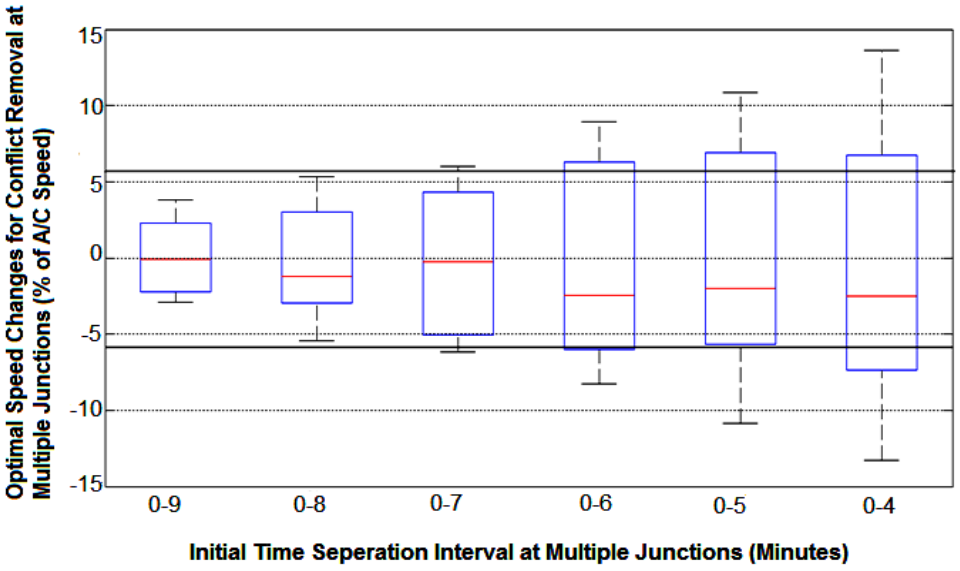

Figure 17.Statistics for the required speed changes to resolve conflict at multiple conflicted junctions for different randomized time separation intervals between consecutive A/C, involving a bunch of 6 A/C arriving at the first junction and 3A/C arriving A/C at the second junction

The performance of the proposed method provides the expected results and, although the optimization tool has scalability problems when applied to high traffic environments, as a LP is applied, the foreseen execution times are not expected to be a limiting factor.

4.10 Complexity at the junctions

Strategic a priori removal of expected conflicts among planned A/C trajectories, identified and mitigated in a centralised manner, does not ensure “free of conflict” to the actual flown trajectories. This can be due to the appearance of additional unexpected events (not embedded into the previously considered stochastic characterisation) or whether because the current situation is beyond the chosen limiting boundaries (outliers).

Under any of the above situations the ATC system has to be able to maintain the required safety levels by applying reactive actions. This capability strongly depends on

the available resources devoted to cope with them at that time and on the complexity of the new scenario. The complexity of the airspace is changing in time and location, and therefore, it has to be continuously monitored and mitigated, helping to employ the ATM capabilities to properly react in the most safe and efficient manner.

Modelling the air traffic complexity is beyond the scope of this paper. The concept used in this work is taken from previous studies.[33,34] From these two studies, two main concepts are retained here for further elaboration; air "traffic density" and "intrinsic complexity".

The pursued purpose is to associate a complexity indicator to any (active) junction, generated by the involved and surrounding A/C under nominal and even reference conditions. This assessment completes the information required to support a planning process within traffic flow management. In other words, it will reveal whether the involved junction should be declared a "hot spot" (that is; showing high complexity) and subsequently it will then be considered as a situation requiring special ATM attention and resources.

The definition of these two parameters uses the junction's coordinates (3D), and additionally the "time of interest". The latter (referred as t_{m0} for junction m) is established as mean time among all modified (by small speed changes) expected TOA to the junction (${t^+}_{mi}$) for the A/C (i) among all the involved arriving A/C (N_m) (Here it has been assumed that a finite and small number of A/C are arriving to the junction with a time interval below the minimum required):

$$t_{m0} = \frac{\sum_i t^+_{mi}}{N_m} \quad (35)$$

Once defined both, coordinates and time of interest (t_{m0}), the traffic density (D_m) and the intrinsic complexity (I_m) are computed for time t_{m0}. The traffic density is defined as superficial relative density, this changes the approach proposed by Delahaye and Puechmorel[35] to:

$$D_m = R^2 \sum_{n=1}^{N} \frac{1}{\max(d_{mn}, R/2)^2} \quad (36)$$

Where d_{mn} is the distance between the A/C (n) position and the junction (m) and R is the characteristic distance used for the definition of the surrounding area. To avoid singularity in Equation (36) when $d_{mn} \to 0$, then if $d_{mn} \leq R/2$, the value $R/2$ is considered instead. The sum shall consider all A/C (N) within a given ratio (say, $3R$) giving representative changes on the relative density value.

The Intrinsic complexity is adopted from the work presented by Delahaye and Puechmorel, [36] where the air traffic surrounding the junction at that reference time (t_{m0}) is modelled as a local linear dynamical. The idea of this approach is to model the set of N A/C trajectories in this vicinity by a flow evolving like a dynamical system defined by the following equation:

$$\dot{X} = f(X)$$

Where $\dot{\boldsymbol{X}}$ and $\boldsymbol{X}$ are respectively the speed and position of the A/C. In the surrounding area of the junction m, located at $\boldsymbol{X_m}$ and assuming existence of the first spatial derivatives, the equation above can be rewritten as:

$$\dot{dX} = J_f \, dX \quad (37)$$

Where $\boldsymbol{J_f}$ represent the Jacobian matrix for the function $\boldsymbol{f}(\boldsymbol{X})$ at point $\boldsymbol{X_m}$. Then, assuming smooth behaviour of $\boldsymbol{f}(\boldsymbol{X})$ it can be approximated by:

$$\dot{\boldsymbol{X}} - \dot{\boldsymbol{X_m}} = \boldsymbol{J_f}(\boldsymbol{X} - \boldsymbol{X_m}) + \boldsymbol{HOT} \approx \boldsymbol{J_f}(\boldsymbol{X} - \boldsymbol{X_m}) \quad (38)$$

By taking $\boldsymbol{X_m}$ as the origin, Equation (38) becomes:

$$\dot{\boldsymbol{X}} \approx \boldsymbol{J_f} \cdot \boldsymbol{X} + \dot{\boldsymbol{X_m}} \quad (39)$$

Variable *X* now represents the coordinates of the A/C in the proximity of the junction and $\dot{\boldsymbol{X}}$ the speed of the "flow of A/C" at this point. The normal terminology for linear dynamical systems is used by calling **A**=$\boldsymbol{J_f}$ and **B**=$\dot{\boldsymbol{X_m}}$, the homogenous part of Equation (39), ($\boldsymbol{A} \cdot \boldsymbol{X}$) exhibits the dependence of the velocity on the A/C position, whereas the independent part ($\boldsymbol{B}$) represents the drift or velocity for the A/C flow at $\boldsymbol{X_m}$.

The real part of the eigenvalues for $\boldsymbol{A}$ matrix are related to the convergence or the divergence property of the traffic flow at the junction. When the eigenvalue has a positive real part, the flow in the correspondence eigenvector is considered in expansion and when it is negative the flow is considered in contraction. Furthermore, the imaginary part provides information on the level of curl organization of the flow dynamic.

The Least Mean Square regression is applied in order to extract the best estimate for matrix $\boldsymbol{A}$ and vector $\boldsymbol{B}$. Based on the observations of A/C (positions and speed vectors), the dynamical system model is adjusted. For each A/C (n), it is supposed that the position ($\boldsymbol{X_n}$) and its velocity ($\boldsymbol{V_n}$) are given. An error criterion between the system model and the observations is used to define the cost function (L) to be minimised as:

$$L = \sum_{n=1}^{N} \|\boldsymbol{V_n} - (\boldsymbol{A} \cdot \boldsymbol{X_n} + \boldsymbol{B})\|^2 \quad (40)$$

From this equation, the $\boldsymbol{A}$ matrix is derived.

The eigenvalues of matrix $\boldsymbol{A}$ are used to compute the intrinsic complexity. The greater their negative real part, the higher degree of convergence to the junction for the existing air traffic which indicates a worse scenario. In addition, their imaginary part represents the traffic vorticity which involves a more complex situation. When the topology of the scenario was introduced (see **Figure 1**), it was assumed that internal nodes included the whole TMAs. Traffic inside this airspace is the one where a higher degree of vorticity are expected, therefore, in order to simplify the approach only the real part of eigenvalues of matrix $\boldsymbol{A}$ are retained for the definition of the proposed intrinsic complexity indicator. In the same way, the eigenvectors provide the "main directions" (in average sense) from where the incoming traffic is arriving to the junction with a characteristic time established by its eigenvalue ($-\frac{1}{real(eig(k)}\ s$, in unit of time).

The degree or time of convergence, represented by the opposite of the inverse of the real part of eigenvalues of matrix $\boldsymbol{A}$ ($-\frac{1}{real(eig(k)}\ s$), is then compared to the expected

reaction time for the ATC system (T_{ATC}, which is in around few minutes). The pursued result shall provide a relevant indicator on the ratio between the traffic convergence time and the ATC required reaction time (T_{ATC}), representing the severity of the situation. Therefore, $-T_{ATC}.real(eig(k)) > 1$ represents strong severity situations, whilst the smaller ratios give a more relaxed scenario. Furthermore, the proposed intrinsic complexity indicator (I_m) at the junction (m) is defined as an exponential function of the real parts of the three eigenvalues for matrix $\boldsymbol{A}$ (k):

$$I_m = \sum_{k=1}^{3} e^{-T_{ATC}.real(eig(k))} \quad (38)$$

The final chosen complexity indicator (C_m) for junction m is then built by multiplying the traffic relative density (D_m) as defined in Equation (36) and the above intrinsic complexity (I_m), assuming that$N \geq 2$:

$$C_m = \left[R^2 \sum_{n=1}^{N} \frac{1}{\max(d_{mn}, R/2)^2}\right] \cdot \left[\sum_{k=1}^{3} e^{-T_{ATC}.real(eig(k))}\right] \quad (39)$$

It is important to establish a threshold to differentiate those (active) junctions representing “hot spots” from the others representing “normal” scenarios, demanding only small TOA changes. To this end, a characteristic distance $R = 5NM$ and ATC reaction time $T_{ATC} = 2\ min$ are assumed.

Then, the proposed threshold is chosen as the equivalent to that used to trigger the existence of a “traffic alert” event between two A/C within a typical ATC-RDPS-STCA

algorithm. Values for the STCA characteristic time and relative distance for the intruder A/C are around: $T_{STCA} = 90s$ and $d{\sim}15NM$ leading to the following value for the complexity (Equation 39):

$$C_m = \left[4 + \frac{1}{9}\right] \cdot \left[e^{T_{ATC} \cdot \frac{1}{T_{STCA}}}\right] \approx 16$$

From this result, it is considered that any junction having the complexity (C_m) higher than the above number will be classified as "hot spot".

The exponential behaviour of Equation (39) regarding the convergence of traffic (represented by the last factor), produces a very fast grow result when the characteristic time ($-\frac{1}{real(eig(k))}$) drops below the ATC's typical reaction time (T_{ATC}). For instance, taking the conditions for TCAS TA time ($T_{TCAS} \approx 48\ sec$) and distance between A/C ($d \approx 5\ NM$), the resulting complexity (C_m) raises up to 60, almost four times the established threshold. As a comparison, for a TCAS RA situation, the complexity value is above 246.

The identification of a junction as "hot spot" is here interpreted as situations where subliminal TOA changes are not enough to remove conflicts or, in other words, indicate that some required speed changes are above any realistic value.

Further developments of this concept will complete the assessment of any TOA change, providing the initial and resulting complexity, during the evolution of the traffic through the junction. This information about the junction as hotspot should be used as

complementary information to finally decide the best measure to cope with the final ATFCM measure.

5 Conclusions

Implementation of direct routes and free routing airspace, applied to high density airspace, are changing the traffic flows patterns, forcing both, ATFCM and ATC, to change. ATC sector occupancy and dynamic sectorisation are some steps in that direction, but they are still anchored in the conventional concept “airspace based operations” rather than in the new one “TBO”. This paper postulates a new metric for the demand measure, based on hotspots and, as well, derives a method for establishing the corrective actions to mitigate them at strategic level, fully aligned with the TBO concept.

Hotspots are here defined as “active” junctions, where a bunch (of at least two) flights are expected to cross their trajectories with less than a well-defined minimum time interval, demanding a special attention by ATC and, likely to produce reactive corrective actions. Based in the initial RBTs, these hotspots are identified by the NM, this identification includes the expected TOAs for the involved A/C. The minimum “safe” time interval has been derived in this paper and, for a given set of conditions, is established to be 9.5 minutes.

The ATFCM mitigation actions are based on establishing the new TOA to the junctions for all A/C that remove conflicts, considering all potential space-temporal interdependencies. The computation of these times is based on basic LP optimization, where the total amount of distance-weighted speed changes are minimized and the initial targeted departure and arrival times are maintained (as constraints). A maximum allowed

speed change is also imposed. These new times shall be issued by the NM to the A/C to be included within the new RBT as requested target times to overfly (TTOs) for crossing points, and target times to arrival (TTA) to TMAs entry points.

The initial results show a good performance in terms of the A/C speed changes feasibility for the proposed TOA changes, and the complete removal of conflicts, and then, of the corrective ATC action under ideal conditions. This behavior has been obtained for different traffic samples, including a relevant junction's overload (up to six A/C arriving at the junction at a rate above the junction capacity) and spatial-temporal interdependencies.

Further work, in terms of the complementary complexity metric, introduced at the end of the paper, is still pending. Furthermore, the behavior of the proposed optimization method, applied to a wider airspace and more realistic traffic sample, has to be also analyzed.

References

1. Zhang W, Kamgarpour M, Sun D, et al. A hierarchical flight planning framework for air traffic management. Proc IEEE. 2012;100(1):179–94.
2. Eurocontrol Performance Review Commission. “Performance Review Report- An Assessment of Air Traffic Management in Europe during the Calendar Year 2016. Draft Final Report for consultation with stakeholders.” 2017;(April).
3. Eurocontrol - STATFOR. 2013 (Dec.). Long-term forecast – flight movements 2012 - 2035. Tech. rept.Eurocontrol, Brussels (Belgium). 1, 2.
4. Majumdar A, Ochieng W. Factors Affecting Air Traffic Controller Workload: Multivariate Analysis Based on Simulation Modelling of Controller Workload. Transportation Research Record: Transp Res Rec. 2002. 58-69 p.
5. SESAR Consortium. The Roadmap for Delivering High Performing Aviation for Europe, European ATM Master Plan. 2015;
6. FAA. Concept of Operations for the Next Generation of Air Transportation System. Tech Rep. 2010;
7. Nieto FJS. The long journey toward a higher level of automation in ATM as safety critical, sociotechnical and multi-Agent system. Proc Inst Mech Eng Part G J Aerosp Eng. 2015;0(0).
8. Richetta O, Odoni AR. Dynamic solution to the ground-holding problem in air traffic control. Transp Res Part A. 1994;28(3):167–85.

9. Vranas PB, Bertsimas DJ, Odoni AR. The Multi-Airport Ground-Holding Problem in Air Traffic Control. Oper Res. 1994;42(2):249–61.

10. Bertsimas D, Patterson SS. The air traffic flow management problem with enroute capacities. Oper Res. 1998;406–22.

11. Bertsimas D, Lulli G, Odoni a. An Integer Optimization Approach to Large-Scale Air Traffic Flow Management. Oper Res. 2011;59(1):211–27.

12. Kuchar JK, Yang LC. A review of conflict detection and resolution modeling methods. Intell Transp Syst IEEE Trans. 2000;1(4):179–89.

13. Vela A, Solak S, Singhose W, et al. A mixed integer program for flight-level assignment and speed control for conflict resolution. Proc IEEE Conf Decis Control. 2009;5219–26.

14. SESAR Consortium, "The ATM target concept, milestone deliverable 3", Version 1.0, 2007;

15. Gawinowski G, Drogoul F, Guerreau R, et al. Erasmus contribution to the 2020 SESAR scenario. AIAA/IEEE Digit Avion Syst Conf - Proc. 2008;1–10.

16. Rey D, Rapine C, Fondacci R, et al. Subliminal Speed Control in Air Traffic Management: Optimization and Simulation. Int J Transp Sci Technol. 2016;50(1):240-262.

17. Drogoul F, Averty P, Weber R. ERASMUS Strategic Deconfliction to Benefit SESAR. Eur Air Traffic Manag Res Dev Semin. 2009;

18. International Civil Aviation Organisation. Time adherence in TBO. 2014;ICAO(October). Available from:

http://www.sesarju.eu/sites/default/files/documents/reports/WP636

19. SESAR P04.07.02 - D22 Preliminary OSED_4, edition. January 2016.
20. Delahaye D, Puechmorel S, Hansman RJ, et al. Air Traffic Complexity Map Based on Non Linear Dynamical Systems. Air Traffic Control Q. 2004;12(4):367–88.
21. Gurtner G, Bongiorno C, Ducci M, et al. An empirically grounded agent based simulator for the air traffic management in the SESAR scenario. J Air Transp Manag. 2017;59:26–43.
22. Gatsinzi D, Nieto FJ , Madani I. "Hot Spot Identification and Mitigation at Strategic Level by Subliminal Changes in Aircraft Time of Arrival at Junction." proceedings of SESAR Innovation ,November 2016, Delft , The Netherlands.
23. iFly project.Complexity metrics applicable to autonomous A/C. Deliverable D3.1. (2009).
24. Sáez Nieto FJ, Arnaldo Valdés R, García González EJ, McAuley G, Izquierdo MI. Development of a three-dimensional collision risk model tool to assess safety in high density en-route airspaces. Proc Inst Mech Eng Part G J Aerosp Eng .2010;224(10).
25. Hilburn B. Cognitive Complexity in Air Traffic Control a Literature Review. EEC note 2004;(04).

26. Sun D, Bayen AM. Multicommodity Eulerian-Lagrangian Large-Capacity Cell Transmission Model for En Route Traffic. J Guid Control Dyn .2008;31(3):616 28.

27. Cao Y, Sun D. A parallel computing framework for air traffic flow management. Proc 2011 Am Control Conf. 2011;2771–6.

28. Day V. The ATC Interactive Radar Simulator Operations Handbook. 2002;(August).

29. Mondoloni S, Swierstra S. Commonality in disparate trajectory predictors for air traffic management applications. In: AIAA/IEEE Digital Avionics Systems Conference - Proceedings. 2005.

30. Commission PR. Performance Review Report. An Assessment of Air Traffic Management in Europe during the Calendar Year 2014. 2015;(March).

31. Team CI, Manager Q, Team CI. SESAR Concept of Operations. 2007;(July):1–214.

32. Mutuel LH, Neri P, Paricaud E. Initial 4D Trajectory Management Concept Evaluation. Eur Air Traffic Manag Res Dev Semin. 2013.

33. Delahaye D, Puechmorel S, Hansman J, et al. Air traffic complexity based on nonlinear dynamical systems. In: ATM 2003, 5th USA/Europe Air Traffic Management Research and Development Seminar. 2003.

34. Prandini M, Piroddi L, Puechmorel S, et al. Toward Air Traffic Complexity Assessment in New Generation Air Traffic Management Systems. IEEE Trans Intell Transp Syst. 2011;12(3):809–18.

35. Delahaye D, Puechmorel S. Air traffic complexity: towards intrinsic metrics. 3rd USA/Europe Air Traffic Manag R&D Semin . 2000;(June):1–11.

36. Delahaye D, Puechmorel S. Air traffic complexity based on dynamical systems. Proc IEEE Conf Decis Control. 2010;2069–74.

Abbreviations

A/C	Aircraft
A-CDM	Airport Collaborative Decision Making
ANSP	Air Navigation Service Providers
ATC	Air Traffic Control
ATCO	Air Traffic Controller
ATFCM	Air Traffic Flow and Capacity Management
ATFM	Air Traffic Flow Management
ATM	Air Traffic Management
ATS	Air Traffic Services
CARD	Conflict And Risk Display
CD&R	Conflict Detection and Resolutions
CNS	Communication, Navigation and Surveillance
CPA	Closest Point Approach
CTA	Controlled Time of Arrival
CWP	Control Working Position
DCB	Demand Capacity Balancing
DMAN	Departure Manager
E-AMAN	Extended Arrival Manager
ECAC	European Civil Aviation Conference
EFPL	Extended Flight Plan
ERASMUS	En-Route Air Traffic Soft Management Ultimate System
FMS	Flight Management System
FOC	Flight Operation Centres
FR	Free Routing

FRA	Free Routing Airspace
FTS	Fast Time Simulations
GDP	Ground Delay Problem
HMI	Human Machine Interface
ICAO	International Civil Aviation Organisation
MILP	Mixed Integer Linear Programme
Navaids	Navigation Aids
NM	Network Manager
PBN	Performance Based Navigation
PRR	Performance Review Report
RBT	Reference Business Trajectory
RNP	Required Navigation Performance
RTA	Required Time of Arrival
SESAR	Single European Sky ATM Research
STAM	Short Term ATFCM Measure
STCA	Short Term Collision Avoidance
TBO	Trajectory Based Operations
TCAS-RA	Traffic Collision Avoidance System-Resolution Advisories
TCAS-TA	Traffic Collision Avoidance System-Traffic Advisories
TC-SA	Trajectory Control by Speed Adjustment
TMA	Terminal Manoeuvring Area
TRACT	Trajectory Adjustment through Constraint of Time
TSE	Total System Error
UDDP	user driven prioritisation process
US	United States
WP	Waypoint

2017-09-03

Development of a new method for ATFCM based on trajectory-based operations

Gatsinzi, Dany

SAGE

Gatsinzi D, Saez Nieto FJ, Madani I, Development of a new method for ATFCM based on trajectory-based operations, Proceedings of the Institution of Mechanical Engineers, Part G: Journal of Aerospace Engineering, Volume 233, Issue 1, 2019, pp. 261-284

http://dx.doi.org/10.1177/0954410017728968